Graduate School Form
30 Updated 12/26/2015

PURDUE UNIVERSITY
GRADUATE SCHOOL
Thesis/Dissertation Acceptance

This is to certify that the thesis/dissertation prepared

By Yizhi Jiang

Entitled

MECHANO-SENSITIVITY OF NUCLEAR LAMIN PROTEINS IN ENDOTHELIAL CELLS

For the degree of Master of Science in Biomedical Engineering

Is approved by the final examining committee:

Julie Ying Hui Ji
Chair

Sungsoo Na

Joseph Wallace

To the best of my knowledge and as understood by the student in the Thesis/Dissertation Agreement, Publication Delay, and Certification Disclaimer (Graduate School Form 32), this thesis/dissertation adheres to the provisions of Purdue University's "Policy of Integrity in Research" and the use of copyright material.

Approved by Major Professor(s): Julie Ying Hui Ji

Approved by: Julie Ying Hui Ji 7/22/2016

Head of the Departmental Graduate Program Date

MECHANO-SENSITIVITY OF NUCLEAR LAMIN PROTEINS IN ENDOTHELIAL CELLS

A Thesis

Submitted to the Faculty

of

Purdue University

by

Yizhi Jiang

In Partial Fulfillment of the

Requirements for the Degree

of

Master of Science in Biomedical Engineering

August 2016

Purdue University

Indianapolis, Indiana

ACKNOWLEDGMENTS

I would like to acknowledge my thesis advisor, Dr. Julie Ji, for guiding me along the research and spending time for my thesis.

I would like to thank my advisory committee members, Dr. Sungsoo Na and Dr. Wallace Joseph, for their time and support throughout my thesis.

I also would like to thank my family members and friends, for their unlimited love and encouragement.

Last but not least, I appreciate and give my best wishes to all that helped and supported me along my thesis.

TABLE OF CONTENTS

Page

LIST OF TABLES

LIST OF FIGURES

ABSTRACT

Jiang, Yizhi. M.S.B.M.E, Purdue University, August 2016. Mechano-sensitivity of Nuclear Lamin Proteins in Endothelial Cells. Major Professor: Julie Ying Hui Ji.

Atherosclerosis is a chronic disease that happens mostly in aged people, and recently studies have showed many similarities between Hutchinson Gilford Progeria Syndrome (HGPS) cells and aging cells, implicating dysfunctions of lamin A/C in aging process and atherosclerosis, as HGPS is caused by a mutated form of lamin A/C.

Blood flow in arteries is generating shear stress that is mostly applied on endothelial cells that align along inner blood vessel wall. At the same time, endothelial cells are also under stretch by periodic arterial pulses. Considering the fact that atherosclerosis is prone to developing at arterial branches with disturbed shear and increased stretch, it is highly possible that laminar flow and proper stretch force are regulating endothelium to function appropriately.

In this thesis, the investigation of what effects laminar flow or cyclic stretch can bring to endothelial cells was conducted, and examination of lamin A/C expression under mechanical forces were elaborated and incorporated with cell senescence. Results showed that laminar shear stress and stretch force can regulate lamin A/C expression in different patterns, which were impaired in senescent cells.

1. INTRODUCTION

This thesis will begin with background information on cardiovascular biology, endothelial mechano-biology, as well as nuclear lamins, laminiopathies, and aging in an overview of the literature. The specific objectives of the thesis project will be presented. Subsequent sections of the thesis include Materials and Methods, Results, Discussion. A summary of conclusions and significance of this project will be presented, and the future research direction will be discussed.

1.1 Cardiovascular Diseases and Atherosclerosis

Cardiovascular disease has become the leading cause of death in developed world. It is a disease of the circulatory system that is influenced by many risk factors, such as obesity, unbalanced diet, abuse of tobacco or alcohol, hypertension [1], etc. In the cardiovascular system, the disorder that happens at arteries is most severe, and can lead to heart attack or stroke, resulting in death. Ongoing research is helping to understand the molecular mechanisms of cardiovascular disease.

Arterial wall is recognized as three layers that have very distinct components. The inner layer (tunica intima) is a monolayer of endothelial cells residing on a basal membrane, and it is the first layer for sensing chemical and mechanical stimuli from blood flow. The middle layer (tunica media) is made of smooth muscle cells (SMC) and elastic fibers to sustain the hemodynamic forces created during cardiac cycle, and to change artery diameter due to applied pressure. The outermost layer (tunica adventitia) mainly contains fibroblasts and connective tissues to anchor artery to its surrounding tissue, as well as some perivascular nerves for vasodilator and vasoconstrictor effects [2]. Some recent studies have pointed out that the adventitia may also participate in cell-to-cell signaling during arterial injuries [3].

Arterial disorders often start with atherosclerosis, which is a chronic inflammation progress that occurs on artery walls. It begins with the chronic accumulation of oxidized low-density lipoprotein (LDL) in the endothelial cell layer at inner wall of blood vessels [4]. After the excess accumulation of LDL, leukocyte (white blood cell) is recruited and penetrates into the intima to uptake the modified LDL [5]. Then the proliferation and migration of smooth muscle cells as well as degradation of original extracellular matrix components (elastic fibers and collagen) are promoted by mediators. Over time, an atherosclerotic plaque complex that consists of fibrous tissues, fatty substances and cellular wastes will build up on the lesion, which gradually narrows the blood vessel where it resides on. The process can be briefly summarized in Figure 1.1. The blockage is not only influencing the absorption of nutrient and elimination of cellular wastes of its surrounding tissues, but once it ruptures, the resulting thrombus at some vital arteries will fully block the blood supply in that area, which can lead to fatality. Depending on where the thrombus occurs, different types of diseases are classified, such as stroke, where the plaque is cutting off the blood flow in arteries embedded within the brain tissue, or heart attack, where the thrombus is happening at coronary arteries.

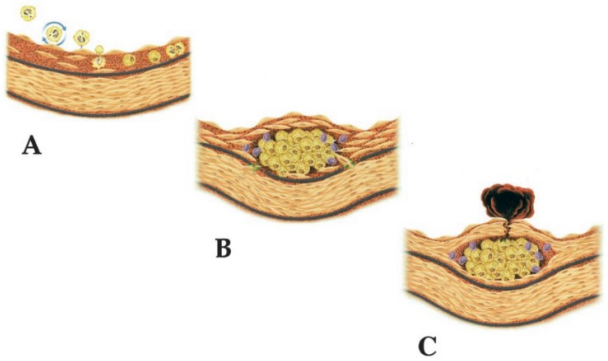

Fig. 1.1. Progression of atherosclerosis. **A.** Leukocyte is recruited to the luminal surface of endothelium. **B.** Foam cells form by uptaking LDL, and SMCs migrate and degrade extracellular components. **C.** Fibrous cap forms and narrows blood vessel, and once rupture, it will potentially cause thrombus. [5]

Recent studies have pointed out the importance of mechanical forces on atherosclerosis formation. A proper mechanical environment may help to prevent the formation of early lesion, as the straight arteries are less prone to lesion formation. At the straight sections of the vasculature, the shear stress and cyclic stretch are more consistent, uni-directional, and less fluctuant than that of branch points or bifurcation sites [6]. Many endothelial molecular pathways have been proved to be regulated by mechanical forces in vascular cells [7–9].

1.2 Endothelial Cells under Mechanical Forces

In the progress of atherosclerosis, endothelial cells play a critical role in responding to mechanical stimuli by means of activating and suppressing intracellular pathways as well as directing larger-scale responses by communications between cells. Considering the mechanical environment that endothelial cells are constantly exposed to, it is highly possible that endothelial cells are very adaptable to extracellular forces, and are able to modify themselves according to different types of mechanical stimuli. Barakat, et al have identified numerous genes and signaling pathways that are activated or suppressed by shear stress ranged from 0 $dynes/cm^2$ to 40 $dynes/cm^2$ [10].

Some studies also addressed pivotal functions that shear stress has on regulating pathways in endothelial cells. For example, tumor necrosis factor alpha (TNFα) is an inflammation promotor that will induce expressions of many proinflammatory factors in endothelial cells. However, when cultured human endothelial cells are kept under shear stress at 12 $dynes/cm^2$ for 16 hours before exposing them to TNFα to induce inflammation, the proinflammatory factors like vascular cell adhesion protein 1(VCAM) were suppressed, other cytoprotective factors were promoted, and they were shown to be regulated through NF-κB pathway [11]. Qi, et al applied low shear stress (5 $dynes/cm^2$) to the primary rat aortic endothelial cells, and they observed that two growth factors - platelet-derived growth factor with two B chains(PDGF-BB) and transforming growth factor β1(TGF-β1) were upregulated in endothelial

cells [12], which can further lead to the enhancement of the migration and proliferation rate of the co-cultured vascular smooth muscle cells, as well as the upregulation of lamin A and downregulation of activated ERK 1/2 and lysyl oxidase(LOX), indicating cell-cell signaling induced by mechanical forces. Moreover, other studies pointed out that atherosclerosis tends to form at branch points within arteries or ostia, where endothelial cells are experiencing disturbed shear stress. Some researchers have also mentioned that endothelial cells can distinguish different patterns of mechanical forces [13]. For instance, Yoshisue, et al have recognized a number of genes whose expressions are enhanced by shear stress in cultured human umbilical vein endothelial cells (HUVEC), and some of them are uniquely expressed according to the pattern of shear stress [14].

Endothelial cells are also recorded to be able to respond to stretch force. Endothelial cells can adjust their cell shapes by realigning stress fibers in order to be elongated perpendicular to the orientation of applied stretch [15]. Lansman, et al reported an increase in the opening frequency of a selective cation channel in endothelial cells after stretched by a patch electrode [16]. Other studies also revealed that stretch can activate adenylate cyclase activity and nitric oxide synthase in bovine aorta endothelial cells (BAECs) after cyclic stretch [17, 18]. However, discriminatory biological responses of endothelial cells from different species were reported, such as the activation of NF-κB, activator protein(AP-1, a transcription factor regulating cell fate), and cAMP response element (CRE) binding protein by stretch force were reported in both HUVEC and human aorta endothelial cells (HUAEC), but those phenomena were not observed in BAEC, which indicates varied responses of endothelial cells from different biological resources, and it poses challenges and barriers for researchers to explore pathways by using cells from difference species.

To sum up, many candidates for mechanotransduction have been proposed and studied. Besides a number of transcription factors, other cellular components like cytoskeleton components, transmembrane proteins such as actin and G protein, as well as mechanosensitive ion channels and focal adhesion [19] have also been proved

to play a part in the comprehensive signaling process. Discoveries of new candidates are still in progress, one of which is lamin A/C, a structural and functional protein in nucleus lamina that will be discussed further in next section.

1.3 Lamins and Laminopathies

Although nucleus is isolated from cytoplasm by nuclear envelope, it is physically connected with cytoskeleton elements through linker of nucleoskeleton and cytoskeleton complex (LINC complex), which is made up of many lamin-associated proteins [20]. Those physical connections provide pathways for force transmission and transduction into nucleus to impact nuclear mechanical properties and gene expression patterns. The inner rim of nuclear envelope is called nuclear lamina. It is composed of nuclear pore complexes (NPC) and lamina network, where A-type and B-type lamins form separate but dependent meshwork. Those lamins work to maintain proper mechanical properties of nucleus, and regulate gene expressions through interactions with various transcription factors or their associated proteins.

A-types lamins (lamin A and lamin C) belong to intermediate filament proteins. They are encoded by the same LMNA gene located at chromosome 1q22 by alternative splicing [21]. However, unlike lamin C, which has a unique 6-amino-acid sequence at C-terminal end, and is directly assembled into nuclear lamina after translation, lamin A needs to go through several posttranslational steps. After translation, the encoded pre-lamin A contains a CAAX motif at the carboxyl terminus, in which the cysteine will be farnesylated afterwards, and -AAX tail will be cleaved with the farnesylated cysteine methylated. Finally, the last 15-amino-acid sequences of lamin A will be cleaved by a metallopeptidase encoded by ZMPSTE24 gene to generate mature lamin A protein. The absence in any of those steps may lead to lamina defects. In order to be incorporated into lamina, those lamins will form a coiled coil dimer, which can associate further together to form a polymer. Two polymers will then combine in an anti-parallel manner to produce a protofilament, which can then associate with

each other to form an intermediate filament with diameter about 10 nm [22]. Those filaments will then interweave within each other to generate an irregular meshwork at the nuclear periphery. Some A-type lamins are not polymerized and are soluble in nucleoplasm, although the role they are playing is still not fully understand.

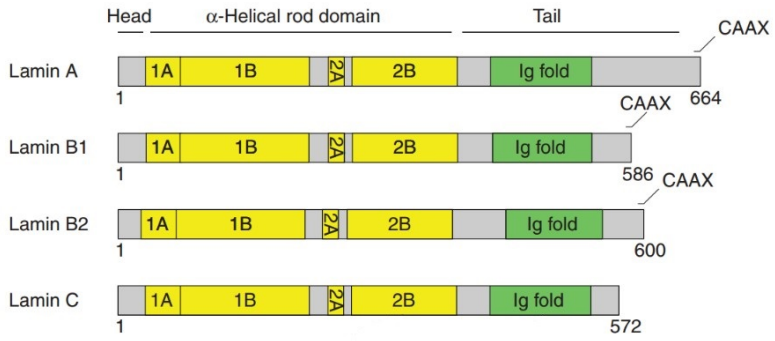

Fig. 1.2. Protein structures of lamins. Both A-type and B-type lamins contain central rod domains (Domain 1A, 1B and 2A, 2B) and an immugolobulin domain. Pre-lamin A have CAAX motif at the tail, but will be deleted after translation. Lamin B1/B2 have CAAX motif reserved in their mature structures [22].

A-type lamins are not the only filamentous network in nuclear lamina. There is another separate meshwork made up of B-type lamins. B-types lamins refer to two proteins - lamin B1 and lamin B2, and they are encoded from different genes - LMNB1 and LMNB2. Although they have similar protein domains as lamin A, such as the central rod domain for polymerization and the CAAX motif, as seen in Figure 1.2, they are expressed ubiquitously in all types of cells, and their farnesylated tails were reserved to anchor them into nuclear lamina all the time. However, A-type lamins are only expressed in differentiated tissues, and they will be disassembled after phosphorylation during mitosis to facilitate chromatin separation. Though lamin A/C and lamin B form separate meshwork, they are not independent and are interacting with each other - some researchers discovered that silencing either lamin B1 or lamin B2 will significantly influence the recovery time of the mobility of lamin A/C in nucleoplasm [23].

Except for the differences in structure, A-type lamins and B-type lamins also seem to have varied functions. Some researchers observed minor nuclear blebbings in mouse embryonic fibroblasts (MEFs) with mutated lamin B1 without observable nuclei mechanical defects. However, for the MEFs with lamin A/C deficiency or lamin C expression only, their nuclear stiffness was reduced compared to wild type MEFs after nuclear strain study [24]. And more and more evidences have shown that lamin A/C is more than a supportive structure. For example, while deleting all B-type lamins from mouse embryonic stem cells can directly cause death, which suggests that it is a pivotal gene in individuals, lamin A/C deficiency or missense mutations in LMNA gene seem to be less lethal at the beginning. However, as the individual develops, many abnormal phenotypes, primarily occur in mesenchymal tissues will appear, which include degeneration of muscular, fat tissue and axon in peripheral nerves, dilated cardiomyopathy, etc [20]. Those tissue-specific disorders implicate the potential essential functions of lamin A/C in regulating cellular pathways besides maintaining nucleus integrity.

Recent studies have unraveled many pathways that lamin A/C is involved in. MAPK/ERK pathway, which acts to transmit and transduce signals from extracellular region into nucleus to further regulate gene transcription, is deteriorated in patients with dilated cardiomyopathy and muscular dystrophy [25]. Researchers also found that in cells with mutated lamin A/C, the disturbed nucleus will excessively activate the ERK 1/2 (extracellular signal-regulated kinases), resulting in increased cell proliferation and migration rate [26]. For patients with lipodystrophy, there is evidence showing that the adipogenesis regulation pathway is impaired, where its transcription factor peroxisome proliferator-activated receptor γ (PPAR-γ) is controlled by β-catenin and emerin [27]. Other transcription factors like retinoblastoma gene protein (pRb), sterol regulatory element-binding protein 1 (SREBP1), Fos, etc. were also reported to be regulated by lamin A/C. Also, evidences of direct binding between A-type lamins and heterochromatin demonstrate the potential ability of lamin A/C to regulate gene expression [28].

1.4 Nuclear Lamins in Aging

Among the diseases caused by dysfunctional A-type lamins, which are known as laminopathies, Hutchinson Gilford Progeria Syndrome (HGPS), a premature aging disease has brought a lot of attention in recent decades. Patients with HGPS often appear normal at birth, but will show accelerated aging after few years. They have aged looks, delayed growth, and often die at their teens by progressive atherosclerosis [29]. The most common mutation in HGPS patients is the heterozygous C1824T at exon 11 at LMNA gene [30], which leads to a 50-amino-acid truncation within the prelamin A. The truncated area contains the sequence that ZMPSTE24 recognizes for the final 15-amino-acid deletion. Therefore, the final protein product - progerin still possesses the last 15 amino acid with the last farnesylated and methylated cysteine at C-terminal after completing posttranslational steps. The farnesylated tail in progerin will cause it to attach to the nuclear periphery permanently, resulting in nuclear mechanical defects and mitotic impairment.

What is notable for HGPS is that, it shares many similarities with normal aging. Progerin was reported to accumulate in human dermal fibroblasts over ages, although its mRNA level remains low in individuals at all ages [31]. Moreover, the same trend was also observed in vascular smooth muscle cells with either high passage or from old donor. Moreover, the overexpression of progerin can result in DNA damage, indicating the acceleration of cell senescence [32]. One study found out that, both old and HGPS dermal fibroblasts showed similar irregular nuclear shapes and DNA damage, which is indicated by increased amount of modified histone [33]. At the same time, those defects were reversible by restoring lamin A expression in both HGPS cells and aged cells [33]. Furthermore, progerin was detected within various tissues in old healthy individuals, while in young individuals it was undetectable. And reduced expressions of A-type lamins were observed in differently types of cells over aging, such as osteoblasts, dermal fibroblasts and cardiomyocytes [34, 35].

All of those findings indicate the importance of lamin A during aging process. Some researchers proposed that the mechanism is due to mechanical defects of nucleus that were cause by progerin, while some papers emphasized several pathways that were deteriorated by mutated lamin A, which indicates gene regulation disorganization in aged cells. In reality, the result is mostly likely led by the combination of those two effects.

1.5 Lamin A/C in Mechanotransduction

To explore how lamin A/C affects mechanical properties of nucleus as well as gene regulations, a lot of efforts have been invested to examine its impacts. On one hand, many mechanical failures of nucleus brought by lamin A/C deficiency were reported. Cells with lamin A/C knockdown were unable to stiffen in response to strains, which indicates the determination of lamin A/C in nuclear stiffness [36]. Moreover, by applying tension on LINC complex after isolating nucleus, the recruitment of lamin A/C was detected, but B-type lamins were not recruited, implicating an unique force-induced connection between LINC complex and lamin A/C [37].

Lammerding, et al assessed nuclear sensitivity after applying cyclic strain on wild-type or lamin A/C-deficient mouse embryo fibroblasts, and results showed that, both nuclear and cytoskeletal stiffness were decreased in lamin A/C deficient cells, which indicates that the stiffen effects on nucleus were not cause by direct force transmission [36]. Moreover, the 10%, 1 Hz cyclic strain can cause the portion of apoptotic cells to elevate, which also indicates that the strain is acting as a mechanical stimulation to affect cell fates. They also found that the pathways for expressing two mechanosensitive genes - egr-1 and iex-1 induced by strain were affected by lamin A/C deficiency. As those genes are regulated by transcription factor NF-κB, further examination for activities of NF-κB subunits was conducted, and results showed that in lamin A/C deficiency cells, the transcription of NF-κB was impaired after transcription factor binding.

Han, et al evaluated lamin A expression and its effects on several transcription factors in primary rate aortic endothelial cells after applying either low shear stress (5 $dynes/cm^2$) or normal shear stress (15 $dynes/cm^2$). They observed that, both lamin A and nesprin2 (a component of LINC complex at nuclear envelope) were down-regulated by low shear stress, and this trend can lead to increased apoptosis and proliferation rate in endothelial cells [38]. Furthermore, when the activation of transcription factors- AP-2 and TFIID as well as suppression of several Stat transcription factors were observed in cells after low shear stress, the overexpression of nesprin2 or lamin A can reverse the former and latter effects, respectively. Considering the specific regulation that lamin A/C control through transcription factors, lamin A seems to be able to regulate cell behaviors and cell fates.

From the above we can conclude that, lamin A/C is a key factor in determining nuclear integrity and regulating cellular pathways in response to forces. On another hand, lamin A/C itself is also potentially regulated by mechanical stimuli, as Han, et al observed. And Swift, et al concluded that lamins expression is scaled with tissue stiffness, which means that stiffer tissue has higher lamin A expression, while in softer tissues B-type lamins dominate [39]. Moreover, they indicated that lamin A expression in response to tissue stiffness is regulated by Retinoic Acid (RA) pathway, in which the transcription factor - retinoic acid is able to bind to the RA-responsive elements (RARE) in LMNA gene. Interestingly, the RARB (retinoic acid receptor-beta), which is activated by RA, is significantly decreased with lamin A deficiency, suggesting that lamin A is in turn regulating RA pathway. Another notable point is that, lamin A seems to act like a viscous material to prevent nucleus rupture by abrupt forces, while lamin B is more of an elastic network.

Overall, lamin A/C is not only an essential dynamic supportive filament for nuclear envelope, but it is also a key factor in mechanical pathways. Though many studies have explored its downstream factors that can be influenced and regulated by lamin A/C, there is still no comprehensive evidence showing how lamin A/C itself responds

to various types of mechanical forces, or is there any upstream effector for regulating lamin A/C expression.

1.6 Thesis Objectives

In this thesis project, lamin A/C was emphasized as a target protein that is potentially regulated by mechanical forces, since the lamin A/C forms a supportive network for nuclear lamina, and its deficiency or mutated isoform can result in mechanical defects of nucleus and blockage of specific mechanical-induced pathways. At the same time, because mutation in lamins can lead to HGPS as discussed above, and the mutated progerin is found in aging people, and considering that both HGPS and aging people are prone to developing atherosclerosis, the aging process was included as part of the project.

Throughout the project, the lamin A/C expression was measured in both protein and mRNA levels, and to access cell age, they were classified into young, middle and old cells by population doubling level in order to evaluate them separately.

This thesis project aims to address the following two questions and hypothesis to be demonstrate in this thesis:

1.Does mechanical stress, such as shear stress and cyclic stretch, influence the expression of lamin A/C proteins in be endothelial cells?

Hypothesis: Mechanical stress affects the expression of lamin A/C in endothelial cells.

2. Does the cell aging process play a part in lamin A/C regulation induced by mechanical stimuli?

Hypothesis: As cells age, they are more susceptible to mechanical stress, and as a result, age can affect lamin A/C regulatory pathways induced by mechanical force.

2. MATERIALS AND METHODS

In order to explore the relationship between lamin A/C and mechanical forces, and how aging process impacts lamin A/C expression, a parallel flow chamber and a stretch device were utilized to apply laminar shear and cyclic stretch on a monolayer of bovine aorta endothelial cells. Western blot and real-time PCR were performed to detect the protein and mRNA expression level of lamin A/C, respectively, and immunostaining was conducted to visualize the distribution of lamin A/C within cells as well as verify Western blot results.

2.1 Mechanical Experimental Designs

There are two primary mechanical forces that endothelial cells are exposed to in the lumen of blood vessel wall. One is a tangential friction force generated by viscous blood flow called shear stress, and the other is the circumferential stretch created by the periodic vasoconstriction of the blood vessel, whose orientation is perpendicular to the luminal surface of vessels, as Figure 2.1 shows.

To exert shear stress and stretch force on endothelial cells *in vitro*, the following two separate simulation systems were utilized to apply different forces on cells.

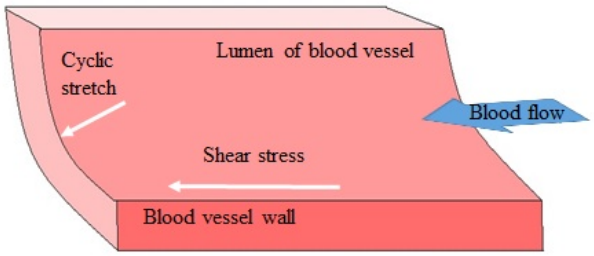

Fig. 2.1. Schematic diagram of part of a blood vessel. There are hemodynamic forces exerted on endothelial cells in blood vessels. Shear stress is tangential along the blood vessel, and stretch is perpendicular to surface of the endothelial cells.

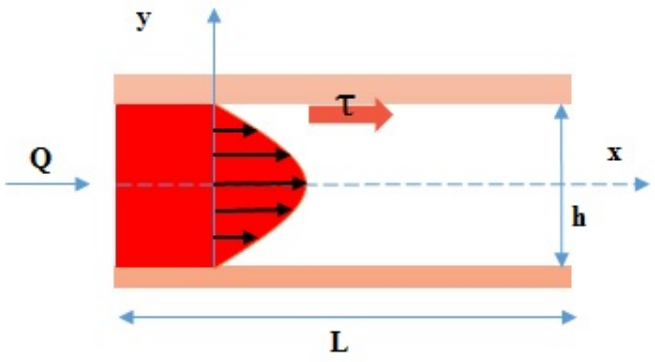

Fig. 2.2. The geometry of the simulated flow area. L is the length of the rectangular flow area, h is the height, Q is the flow rate (volume of flow per unit time), τ is the shear stress generated by the flow, and a Cartesian coordinate system is established to generate equations, where x is crossing the middle layer of the flow.

2.1.1 Shear Stress Experimental Setup

To apply shear stress on cells, a parallel flow chamber was used for shear experiments to produce simplified laminar flow on cells [40]. The geometry of the flow chamber can be described in Figure 2.2, and the calculation of the shear stress generated is briefly shown below.

First of all, Navier-Stokes equation is applied to describe the motion of the fluid considering its viscous property. And as laminar flow is assumed in the flow chamber, therefore only motions in x and y axis are considered as variables, and the equation can be simplified in 2-D as Equation 2.1, where ρ is fluid density, u is the velocity of the flow, μ is the viscosity, p is the pressure applied on the flow.

$$\rho(\frac{\partial u}{\partial t} + u\frac{\partial u}{\partial x} + v\frac{\partial u}{\partial y}) = -\frac{\partial p}{\partial x} + \mu(\frac{\partial^2 u}{\partial x^2} + \frac{\partial^2 u}{\partial y^2}) \tag{2.1}$$

If assuming that flow is along the x axis, and its velocity is symmetric at $y = \frac{h}{2}$, the flow in steady state can be described in Equation 2.2.

$$0 = -\frac{\partial p}{\partial x} + \mu\frac{\partial^2 u}{\partial y^2} \tag{2.2}$$

After integrating twice together with boundary conditions: $u = 0$ at $y = 0$, and u_y=0 at $y = \frac{h}{2}$, the result becomes Equation 2.3.

$$\frac{\partial u}{\partial y} = \frac{1}{\mu}\frac{\partial p}{\partial x}(y - \frac{h}{2}) \tag{2.3}$$

From Equation 2.3, we can derive the maximum velocity u_{max} at $y = \frac{h}{2}$ by integration, which is shown in Equation 2.4.

$$u_{max} = -\frac{1}{8\mu}\frac{\partial p}{\partial x}h^2 \tag{2.4}$$

On the other hand, as shear stress is defined as $\tau = \mu\frac{\partial u}{\partial y}$ in this case, after substituting it into Equation 2.3, it becomes

$$\tau = \frac{\partial p}{\partial x}(y - \frac{h}{2}) \tag{2.5}$$

Also, as the flow rate can be calculated as Equation 2.6, the average flow rate can be calculated as in Equation 2.7.

$$Q = \int_A \overline{V} * \overrightarrow{dA} = -\frac{1}{12}\frac{\partial p}{\partial x}h^3 \tag{2.6}$$

$$\overline{V} = \frac{Q}{A} = -\frac{1}{12\mu}\frac{\partial p}{\partial x}h^2 \tag{2.7}$$

If compared Equation 2.7 with Equation 2.4, we can notice that $\overline{V}$ and u_{max} are linearly related. Moreover, as $\overline{V}$ can also be expressed as

$$\overline{V} = \frac{\dot{m}}{\rho A} \tag{2.8}$$

where $\dot{m}$ is the mass of flow that passes the cross section per unit time, we can incorporate it into Equation 2.4 to express $\frac{\partial p}{\partial x}$, which becomes Equation 2.9.

$$\frac{\partial p}{\partial x} = -\frac{8\mu}{h^2}\frac{3}{2}\frac{\dot{m}}{\rho A} \tag{2.9}$$

Recall the definition of shear stress (Equation 2.5), after substituting $\frac{\partial p}{\partial x}$ by Equation 2.8, we can get

$$\tau = -\frac{12\mu\dot{m}}{h^2\rho A}(y - \frac{h}{2}) \tag{2.10}$$

To incorporate Q into τ, Equation 2.7 and 2.8 were utilized again and the equation becomes

$$\tau = -\frac{6\mu\dot{Q}}{hA} \tag{2.11}$$

Therefore, the strength of shear stress will ultimately depend on the flow rate and viscosity of flow, assuming that the area and height of the flow area is fixed.

In reality, the components of the flow chamber and whole experimental setup are shown in Figure 2.3. As seen in Figure 2.3 A, the bottom piece of the flow chamber (transparent one) has a groove to hold the glass slide, and the middle piece contains two gaskets on each side to prevent media from leaking out. The upper piece has parallel inlet and outlet for media to flow through. Three pieces were assembled together to provide a rectangular flow area for the slide. Twelve screws are to tighten

components together to further prevent media leak. In order to keep consistent experimental conditions, the strength of shear stress was set as 15 $dyne/cm^2$, which was controlled by the comparative height between the chamber and upper tube of the system. Shear time was set as 6 hours. Figure 2.3 B shows the environmental chamber we created to maintain normal growth condition for cells during shearing. A peristaltic pump was used to circulate media from bottom to top reservoir. A heating unit was used to maintain temperature at 37°C, and air with 5% CO_2 was supplied to cells during shearing.

2.1.2 Cyclic Stretch Experimental Setup

To apply stretch force on cells, a stretch device was utilized. This was designed by Dr. Hazim El-Mounayri and his team, our collaborators from Mechanical Engineering Department at IUPUI. The stretch device is shown in Figure 2.4.

Figure 2.4 A shows the chamber holding flexible substrate (silicone membrane) with cells attached. It consists mainly of two arms into which membranes are clipped in place (upper left and lower right corners). Clips, shown in the upper right corner, fixes the membrane on each side of the slider. The membranes sit into a 4-chamber cell culture dish which can be filled with culture media and allow for cell growth, and a clear transparent cover slides over the cell chambers is to maintain the sterile environment through stretch experiment. The two arms then slide into a housing unit that fit into the stretch device (Figure 2.4 B). One arm is held stationary (left side), while the other is attached to a rotor that pulls it in a cyclic at a specified % strain (right side). The motor on the right is connected to the computer, and its movement is programmable and is controlled by CoolWorks Lite 4.1.7.4 software. The entire stretch system (Figure 2.4 B) was maintained in a 37°C incubator with supplement of 5% CO_2 air.

To conduct the stretch experiment, a flexible silicone membrane was used as an alternative substrate for cell attachment. Membranes were coated with fibronectin

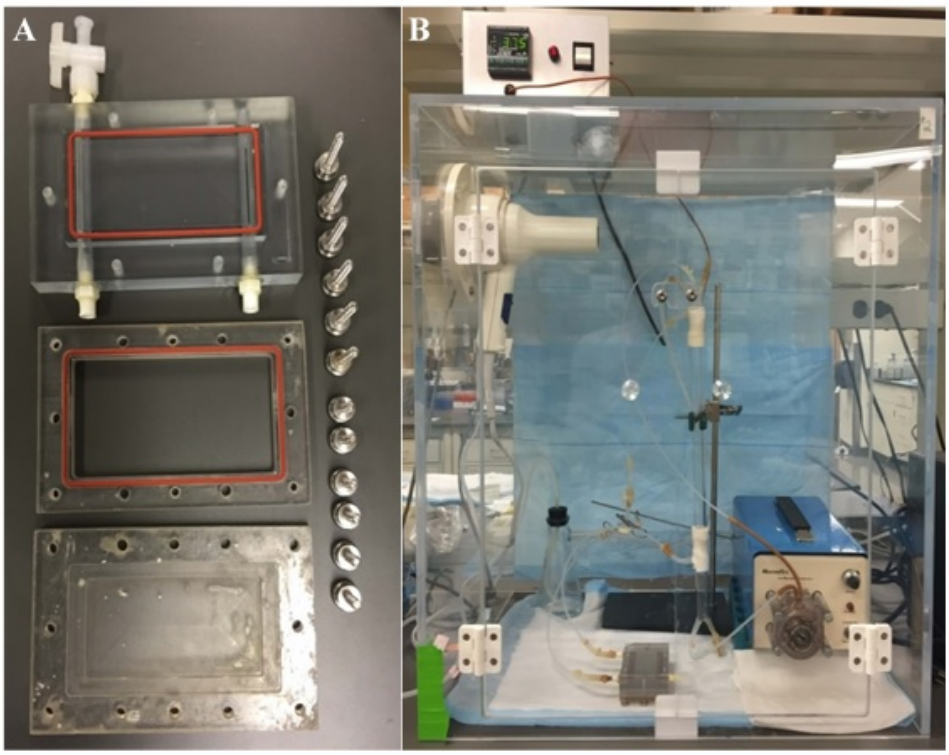

Fig. 2.3. Experimental components for shear stress. **A.** Components of flow chamber. It is made up of three pieces of the cell flow chamber: top, middle, and bottom pieces, and are assembled by 12 screws to hold a glass slide tightly. **B.** Housing environment for shear supplied with 5% CO_2 at 37 °C. Multiple sizes of teflon and silicone tubes, connectors and a tubing pump (Masterflex) are connected properly to build up a circulating system to create a static pressure on flow.

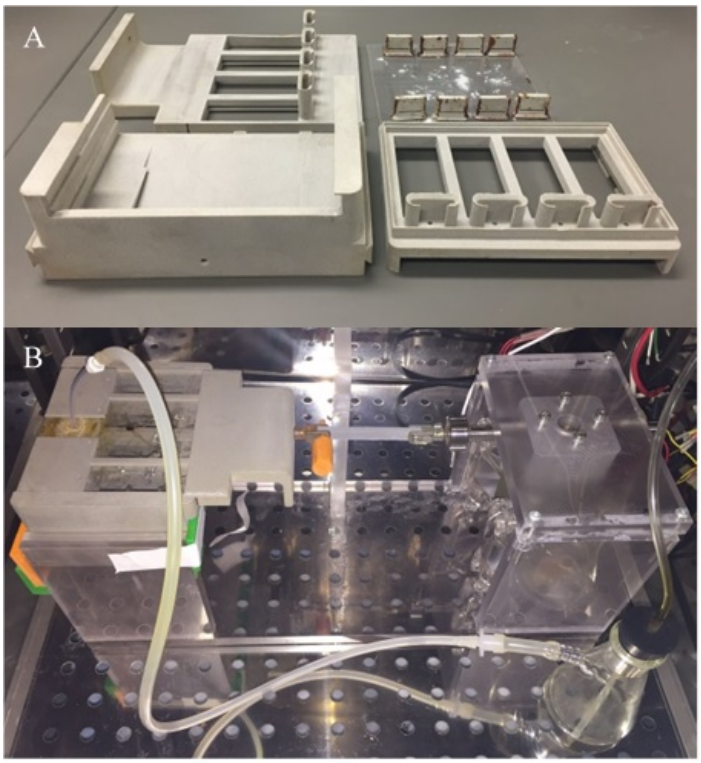

Fig. 2.4. Experimental components for cyclic stretch. **A.** Stretch device. The main stretch parts (upper left and lower right) can hold membranes from the end by clips (upper right). Membranes are kept in a culture dish filled with media. The transparent plate (upper right) is to maintain sterile environment, and they are combined with the base (lower left). **B.** Stretch system. Stretch device is kept stationary on left end, and the right end was connected to the arm of the motor on the right, whose movement is controlled by computer. The system is maintained in a 37 °C incubator with supplement of 5% of CO_2 air.

($2\ \mu g/ml$) prior to seeding cells to assist cell attachment. 1 Hz, 10% of 6-hour cyclic stretch was applied on cells.

2.2 Cell Culture

Bovine aortic endothelial cells (BAEC) were grown in Dulbeccos Modification of Eagles Medium (DMEM, Corning) containing 10% of FBS (Fetal Bovine Serum, JR Scientific), 1% of L-Glutamine (Cellgro) and 2% Penicillin streptomycin (Cellgro). Cells were cultured in T75 flask (Falcon) and maintained in humidified incubator with 5% CO_2 at 37 °C. Media was changed every two days, and subculture was conducted at a ratio of 1:6 when cells were reaching 95% confluency, and cell population was counted by a hemocytometer.

2.3 Population Doubling Level

Population doubling level (PDL) was utilized to indicate cell age, which refers to the times that cells have divided [41]. Assume that N is the final cell population when cells are reaching confluency in the flask, X_0 is the initial amount of cell population, and n is the number of generations that cells have gone through in the flask. If assuming that cells were growing at an exponential growth rate, then $2^n = \frac{N}{X_0}$, which leads to $n = \frac{logN - logX_0}{log2}$. Therefore, the number of divisions can be calculated from N and X_0. Cells were counted before each subculture to get the N and X_0 in each flask, and we chose to call young cells as having PDL of up to 13 after first passage, middle as to have PDL around 45, and old refers to PDL around 60.

2.4 Protein Analysis

Western blot was performed to quantify protein expression in each sample. First of all, cells were washed once with PBS to remove residual medium, then cells were lysed and collected by RIPA lysis buffer (contains 20 mM Tris HCl, 150 mM NaCl, 1

mM EDTA, 0.1% SDS, 1% Triton-X, 1 mM DTT, 0.5 mM PMSF, 150 mM Protease inhibitor in milli-Q water).

The total protein concentration of each sample was measured by bradford assay to adjust the equal amount of loading samples, where coomassie brilliant blue 250 dye (Bio-rad) was utilized to bind to charging groups of the protein so that the dye color can reflect the protein concentration, which was measured by a spectrometer at 595 nm. 1.45 mg/ml of Bovine serum albumin (BSA) and its two-fold dilution solutions were used to generate a linear standard curve, from which the concentrations of unknown samples can be calculated by using linear regression model. Figure 2.5 shows an example of a standard curve, where the x-axis stands for BSA concentration, and y-axis stands for absorbance value at 595 nm.

After adjusting the amount of loading samples, LDS sample buffer and sample reducing agent (Invitrogen) were mixed with adjusted amount of sample, and was boiled at 95 °C for 10 minutes. After that, proteins were unfolded and stained with visible dye, and were ready to be loaded on a precast polyacrylamide gel and run in MOPS running buffer at 190 Volt for an hour.

After electrophoresis was completed, gel was assembled with one PVDF membrane between four blot papers, with each piece pre-wetted by transfer buffer (contains 25 mM Tris base, 192 mM glycine, 25% methanol in water), and a semi-dry electrophoresis apparatus was used to transfer protein from gel to membrane at 25 Volt for 45 mins.

After protein transfer was completed, PVDF membrane was carefully cut into two pieces according to the sizes of target protein and control protein, and was blocked in blotto (5% non-fat milk in PBS with 1% tween) at room temperature for one hour. Then membrane was incubated separately with primary antibodies (anti-lamin A/C antibody, produced in mouse (Cell Signaling, #4777), or anti-actin antibody, produced in mouse (sigma A2066)) as well as secondary antibodies conjugated to HRP (anti-mouse or anti-rabbit secondary antibody (Bio-rad)) by required time and solution, with three-time PBS-T washes on shaker in between. After later incubation

with chemiluminesence HRP substrate reagent to detect the presence of secondary antibody, or its relevant protein on membrane, the membrane was imaged by an imaging system (ChemiDoc XRS+ System, Bio-rad).

To quantify protein expression from the image, Quantity One software was used to calculate the intensity of each band. A rectangular box was drawn around each band, and the area of the box stayed consistent for the same protein. The background was corrected according to the local background of each band. Figure 2.6 is an example of the analysis.

2.5 Quantitative RT-PCR

Transcription is an indispensable process before protein synthesis, during which the information in DNA is copied to mRNA, and only after that will protein be translated and expressed. Similar to translation process, where protein can be either degraded or synthesized by its regulating proteins, the transcription expression levels can also be regulated by many transcription factors in response to many chemical or mechanical stimuli.

In order to examine which level mechanical forces is acting on cells, quantitative real-time polymerase chain reaction (RT-qPCR) was performed to verify the transcription levels of interested proteins in different conditions. First of all, mRNA was isolated from cell samples, then reverse transcription was performed to transcribe mRNA into complementary DNA (cDNA), which acted as templates during later amplification steps during PCR.

2.5.1 RNA Isolation

RNA isolation kit (GeneJET RNA purification kit, Thermo Scientific) was used to purify RNA from cells. Cells were first detached by trypsin from either silicone membrane or glass slides, and were collected with fresh media before proceeding to centrifugation (2100 x g for 5 min). The cells were then resuspended in lysis buffer

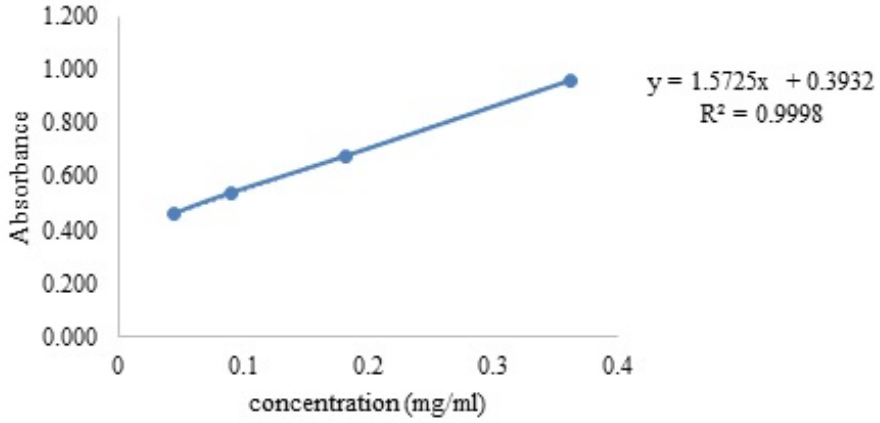

Fig. 2.5. Standard curve of BSA concentration versus its absorbance. Formula on the right describes their linear relationship within the range, and its r-value is very close to 1, which indicates a good fit.

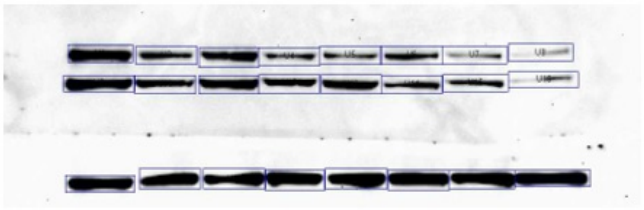

Index	Adj. Vol	Area
1	3328725	278.5583358
2	791842.3	278.5583358

Fig. 2.6. Analysis example of a blot image. Local background subtraction method was selected, and the adjusted intensity was acquired by subtracting the intensity on the peripheral of each rectangular box from its raw intensity, which was done by the software.

with β-mercaptoethanol added to temporarily prevent RNA degradation. Then 95% of ethanol was added and gently mixed by pipetting. After that, lysate was transferred to a provided RNA purification column and was filtered by centrifugation at 12000 x g for 1 minute. After that, RNA will bind to the silica membrane in the bottom of the column in the presence of ethanol, chaotropic salt and the PH provided by the buffer [42]. Then the purification column that contains RNA from the sample was transferred to a new collection tube and washed with wash buffer 1 and wash buffer 2 with supplement of 95% of ethanol to purify the RNA. In the end, RNA was eluted by adding nuclease-free water, and the eluted RNA is ready to use or can be stored at -20 °C.

2.5.2 Reverse Transcription

After obtaining RNA samples, reverse transcription was conducted to generate its cDNA segments. First of all, RNA concentration was measured by NanoDrop spectrophotometer, according to which the amount of sample was adjusted so that 1 μg of RNA was added to be reverse transcribed for each sample. Besides the mRNA template, other necessary materials were provided by a cDNA reverse transcription kit (Applied Biosystem), including reverse transcription (RT) random primers, reverse transcriptase, dNTPs as well as RT Buffer. The amounts of each component in RT mix (total volume is 20 μL) for one reaction were prepared as in Table 2.1.

After reaction mix was prepared, they were loaded on a thermal cycler and underwent three temperature stages to complete reverse transcription, which is shown in Table 2.2.

After reverse transcription was completed, 180 μL of nuclease-free water was added to each reaction tubes in preparation for next PCR step, in which 2 μL of cDNA sample was utilized and amplified.

2.5.3 Real-time PCR

Real-time Polymerase chain reaction (PCR) is a quantitative method for comparing mRNA expression between samples, which is more accurate than normal PCR, since the fluorescence that indicates the amount of synthesized cDNA is detected within each amplification cycle instead of reading the fluorescence only once at the end in the normal PCR [43].

If assuming 100% efficiency for primers, then after each cycle, the amount of cDNA will double after each cycle, i.e. after n cycles, the amount of cDNA will be $m_0 * 2^n$, where m_0 stands for the initial amount of cDNA. To quantify cDNA synthesis number, SYBR green dye (Applied Biosystems) was mixed with cDNA template prior to the reaction, and the dye will bind to double-stranded DNA and emit ration of fluorescence. Therefore, in semi-log plot where the fluorescence is in logarithmic scale, and cycle number is in linear scale, there would be a linear relationship by the exponential amplification, and different samples that start with varied amount of certain mRNA will have their curves shift between cycles. So a threshold (C_t) was set to measure the difference in mRNA, which is the cycle number where a defined fluorescence value was detected. To sum up, more of a certain mRNA is expressed, more of its cDNA will be synthesized, and less cycles it should need to reach the defined amount of fluorescence.

7500 Fast Real-Time PCR device was used to conduct PCR experiment, and the usage of required reagents per reaction is shown in Table 2.3. The amounts of primers for LMNA and GAPDH are different, as LMNA primers are commercially available and are contained in one vial.

Table 2.1
Volumes of components in reverse transcription master mix for each reaction.

Component	**Volume per reaction(μL)**
RNA and nuclease-free water	14.2
10 × RT Buffer	2.0
25 × dNTP	0.8
10 × RT random primers	2.0
Reverse Transcriptase	1.0

Table 2.2
Temperature conditions for reverse transcription

Stages	**Temperature(^oC)**	**Time**
1	25	10 minutes
2	37	2 hours
3	4	hold

Table 2.3
Usage of reagents in one PCR reaction mix

GAPDH	**Per Reaction (μL)**	**LMNA**	**Per Reaction (μL)**
Water	6	Water	7
SYBR	10	SYBR	10
primers	2	primer	1
Template	2	Template	2
Total volume	20	Total volume	20

In reality, as the efficiency cannot perfectly reach 100%, some modifications were made to analyze PCR results. Here Pfaffle method [44] was applied to calculate the results, which considers actual efficiency values in its formula.

Primer pairs for target gene (LMNA) from Bio-rad, use the context sequence: TGAGCCGGGCCTGGGCGGCCATCAGGTCTCCCTCCTTCTTGGAATTGCGTGCCTTGAGCTCCTTGAACTCCTCTCGCACTTTGCTCAGCTCCAGCTGCAGGCGGGCGCGCTCCTTGGCCACCGAGTCAAGGGTCTTGCGG. Primer pairs for control gene GAPDH (Forward primer: 5-GCAAGTTCAACGGCACAGTCA-3; Reverse primer: 5-ACCAGCATCACCCCACTTGAT-3), also commercially available from Invitrogen were used.

2.5.4 Quantitative Analysis

First of all, the efficiency value of each primer was measured by generating a standard curve, where the Ct of 6 samples with 5-fold dilutions were measured and plotted in semi-log graph (with log input), and the efficiency (E) was calculated by the formula [45]:

$$E = (10^{-\frac{1}{slope}} - 1) * 100\%$$

Target gene (LMNA) and control gene (GAPDH) were both measured, E_{LMNA} and E_{GAPDH} were evaluated separately, which turned out to be around 90.35% and 89.72%. Therefore, after n cycles, the fold increase of LMNA and GAPDH are 1.9035^n and 1.8972^n.

To normalize the result in order to compare between samples, the fold increases in target gene (LMNA) and control gene (GAPDH) are integrated in one formula below:

$$Ratio\ of\ increase = \frac{(1+E_{LMNA})^{\Delta C_{tLmna}}}{(1+E_{GAPDH})^{\Delta C_{tGapdh}}}$$

Where ΔC_{tLmna} and ΔC_{tGapdh} denotes differences in threshold between control samples and treated samples after synthesized by primers of LMNA or GAPDH.

Any result that is greater than 1 indicates that the target gene is upregulated after treatment compared with control samples. Each sample was measured three times in triplicate wells to get the average number as well as to eliminate outlier.

2.6 Immunohistochemistry

To access more information on cell morphology and to confirm the Western blot results, immunostaining was conducted to examine the effects of mechanical forces on cells.

First, cells were washed two to three times with PBS, then 4% PFA (paraformaldehyde) was used as fixative for 15 minutes to cross link proteins and maintain cell morphology [46]. To enable antibody to cross cell membrane, 0.2% of Triton-X was used for permeabilization for 10 minutes. After three-time PBS wash, fixed cells were blocked by 1% BSA for an hour to prevent unspecific bindings before antibody incubation or nucleus staining.

For antibody incubation, cells were first exposed to primary antibody of lamin A/C (#4777, cell signaling) at 1:100 dilution in 1% BSA overnight, and then incubated with fluorophore conjugated secondary antibody (anti-mouse antibody with FITC, SC-2099, Santa Cruz) at 1:100 ratio for one hour, and this incubation needs to be conducted in the dark to avoid fluorescent signal loss. Three-time PBS washes were conducted in between to remove unbounded antibodies. After that, cells were ready to be observed under fluorescent microscope or stored at 4^oC in the dark for at most one month.

For nucleus staining, after blocking step, cells were incubated with Hoechst blue stain solutions at 1:1000 dilution for 15 min in the dark, and then washed with PBS three times before proceeding to microscope or 4^oC storage.

2.7 Statistical Analysis

To maintain consistent, every data point was repeated at least three times independently, and cells were treated in the same way. To quantitatively express significant changes, unpaired t-test was performed between two groups, and one-way ANOVA was performed between multiple groups, followed by Turkey-Kramer method, from which P value was acquired. Lower P value means higher possibility that the two sets of samples were different. Data were expressed as mean $\pm$ SEM. And a comparison between samples with P value less than 0.05 was regarded as significant.

3. RESULTS

To evaluate how lamin A/C expression changes through aging process, and how it responds to shear stress or stretch force in terms of different ages, separate mechanical experiments were conducted in young, middle and old cells. Quantifications of lamin A/C protein and mRNA expression levels revealed more details of how lamin A/C is regulated by varied mechanical forces.

3.1 Lamin A/C Expression Pattern Decreases Through Aging Process

We chose to call young cells as having PDL of up to 13 after first passage. Middle cells refer to the cells with PDL around 45, and old cells refer to the cells with PDL around 60. BAEC grown in culture flask were collected by RIPA buffer after each subculture, and Western blot was conducted to quantify lamin A/C expression levels over aging process. The results are shown in Figure 3.1. After normalizing with respect to young cells, the lamin A and lamin C expression levels were 1 ± 0.03, 1 ± 0.06 in young cells, respectively. In middle cells, the lamin A and lamin C expression levels were 0.91 ± 0.231 and 0.78 ± 0.12, respectively. In old cells, the lamin A and lamin C expression levels were 0.32 ± 0.09 and 0.20 ± 0.07, respectively. Figure 3.1 shows the Western blot images and the corresponding quantification results for lamin A/C through aging process, in which the old BAEC shows significant decrease in lamin A/C protein expression (** $P < 0.01$ and *** $P < 0.001$ compared to young cells).

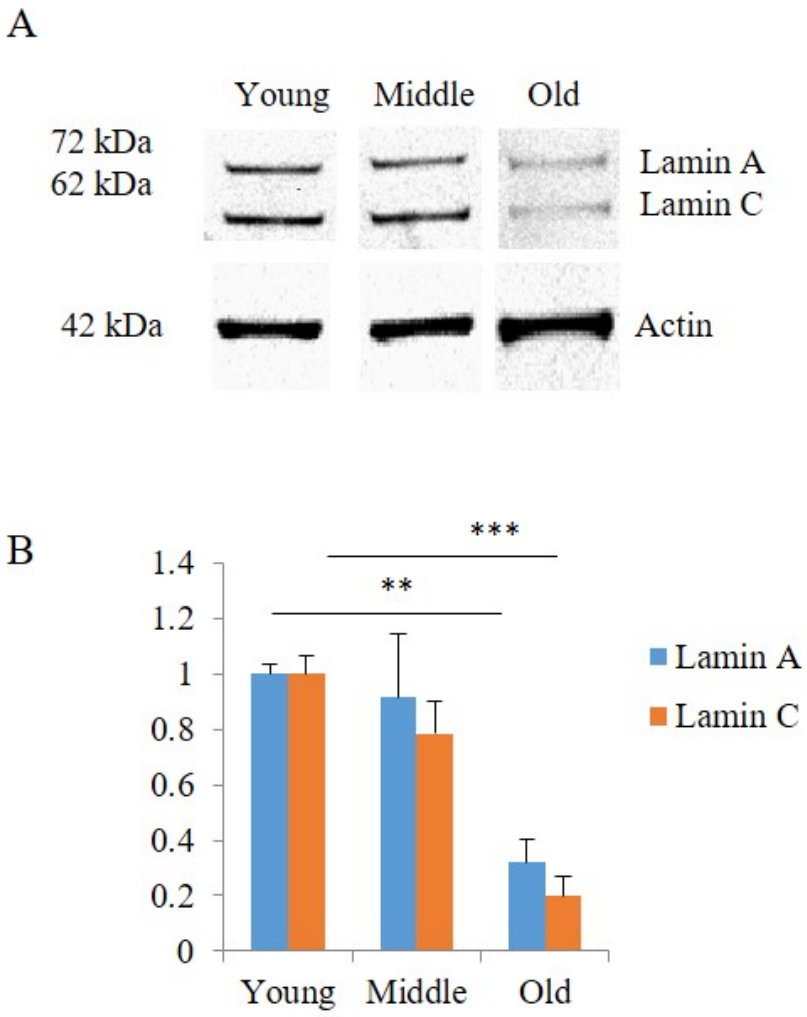

Fig. 3.1. Expression levels of lamin A/C in BAEC in terms of ages. **A.** Representative Western blot for lamin A/C, and actin. **B.** Quantitative results of repeat Western blots. Both lamin A and lamin C showed significant decreases in older cells (**$P < 0.01$ and *** $P < 0.001$ compared to young cells for lamin A and lamin C, respectively). Actin was used to normalize lamin A/C expression, and all data points were normalized to young cells for lamin A and lamin C, respectively.

3.2 Lamin A/C Distribution Becomes More Localized at Nuclear Periphery with Age

Except for the quantitative change in expression levels, we also observed the changes in the distribution of the lamin A/C proteins at the nuclear periphery under static states. To quantify how lamin A/C locates within the nucleus, immunostaining analysis was performed to calculate the ratio of lamin A/C at periphery over the whole nucleoplasm (including the periphery). To keep consistency, the intensity at the periphery was acquired by averaging four points, two of which were picked on the Ferets diameter while the other two were picked on the line that is perpendicular to Ferets diameter and crossing the center of the diameter. The results show that the ratio increases through aging process (*** $P < 0.001$ for old cells compared to either control young cells or control middle cells, as in Figure 3.2). The data for young, middle and old cells were 0.94 ± 0.003, 0.95 ± 0.001 and 0.99 ± 0.001, respectively.

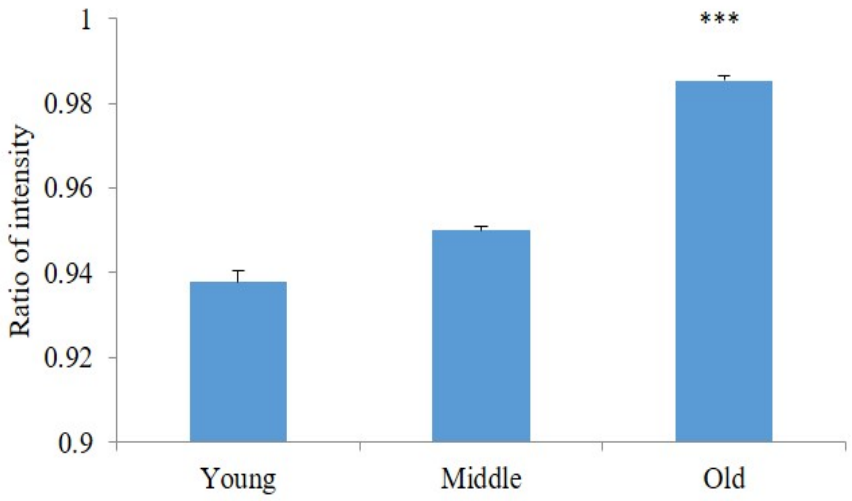

Fig. 3.2. Ratio of lamin A/C intensity at periphery over whole nucleus as aging proceeds. Old cells showed higher ratios of intensity (*** $P < 0.001$ compared to either young or middle cells).

3.3 Nuclear Shape Is Modulated After 6-hour Shear Regardless of Cell Age

We also examined the effect of shear stress on lamin A/C expression in BAEC firstly regardless of cell age. The cells were seeded on glass slides and were exposed to 15 $dyne/cm^2$ of shear stress for 6 hours. Another slide that has been plated and treated the same way was placed in incubator as a static control. After shear experiment, cells were lysed and collected by cell scrapper, and were followed by Western blot. In these cases, the samples were normalized with respect to static control cells. Result in Figure 3.3 shows that the area, circularity and elongation were changed after 6-hour shear, indicating that the nuclear shape was modulated after applying 6-hour shear on cells.

To visualize how BAEC adjusts their nucleus shape during shear, we stained cell nucleus by Hoechst fluorescent stain after shear experiment. By calculating shape factors (area, elongation and circularity) among samples, significant changes were quantified in Figure 3.3, where elongation and circularity were calculated by the following formulas:

$$Elongation = \frac{\pi * Feret's\, diameter}{perimeter}$$
$$Circularity = \frac{4\pi * area}{perimeter^2}$$

We calculated for a minimum of 50 nuclei in both static and shear case. All of those parameter show significant changes after shear (Figure 3.3). In control samples, the area, elongation and circularity were 115.89 ± 3.97, 1.09 ± 0.01, 0.86 ± 0.004, respectively. After shear stress, however, those parameters were 104.74 ± 2.72, 1.13 ± 0.01 and 0.83 ± 0.01, in which the area and circularity significantly decreased after shear ($^*P < 0.05$ and $^{***}P < 0.001$ compared to static cells), and elongation showed significant increase after shear ($^{**}P < 0.01$ compared to static cells). Cells are pooled together for Figure 3.3. Aging effect was not considered here. Instead this data highlights simply the effect of shear stress along on nuclear shape changes.

The increase in elongation and decrease in circularity is consistent with other people's findings following shear stress [47].

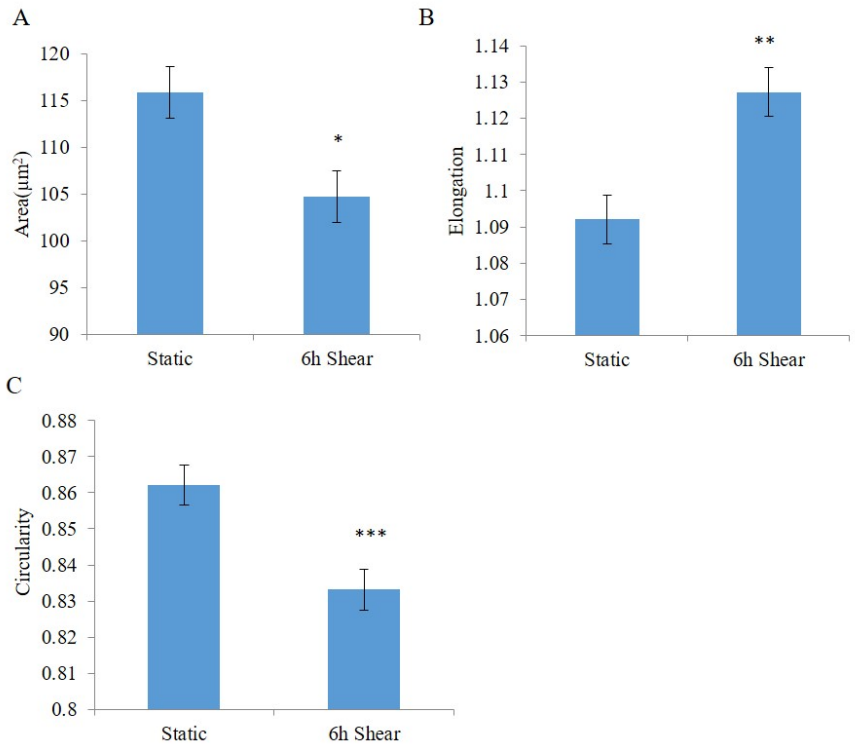

Fig. 3.3. Nuclear morphology analysis after shear regardless of PDL. At least 50 nuclei were assessed for each bar. There shows area **(A)**, elongation **(B)** and circularity **(C)** changes of cells after 6-hour shear. Cells were stained by Hoechst stain solution. Significant decrease in area (* $P < 0.05$ compared to static cells) and circularity (*** $P < 0.001$ compared to static cells), and the increase in elongation (** $P < 0.01$ compared to static cells) were observed. Aging effect was not considered here.

3.4 Protein Expression of Lamin A/C Responds to Shear Stress Differently Through Aging Process

Then we would like to take into account the possible effects brought by aging process. Therefore, we separated young, middle and old cells, and treated them with shear stress individually. The results are shown in Figure 3.4. For young cells, the lamin A and lamin C expression levels decreased significantly after shear stress. Lamin A/C levels were 0.34 ± 0.14 and 0.22 ± 0.04, respectively compared to static, which were 1 ± 0.14 and 1 ± 0.12, respectively (Figure 3.4A). For middle cells, the lamin A/C expression levels after shear were 0.60 ± 0.13 and 0.61 ± 0.14, and the corresponding static samples were 1 ± 0.10, 1 ± 0.06, respectively (Figure 3.4B). While lamin expression increased for young and middle cells, we observed a different trend for older cells. Here, the lamin A/C expression levels were 1.70 ± 0.47 and 1.18 ± 0.06, compared to 1 ± 0.05 and 1 ± 0.10 in control old BAEC, respectively (Figure 3.4C). As Figure 3.4 shows, the lamin A/C decreases in response to shear stress in young cells (* $P < 0.05$ for lamin A and ** $P < 0.01$ for lamin C compared to control young cells), however, this trend dissipates through aging and were inversed in old cells, where the lamin C protein expression indicates an increase (* $P < 0.05$ compared to control old cells).

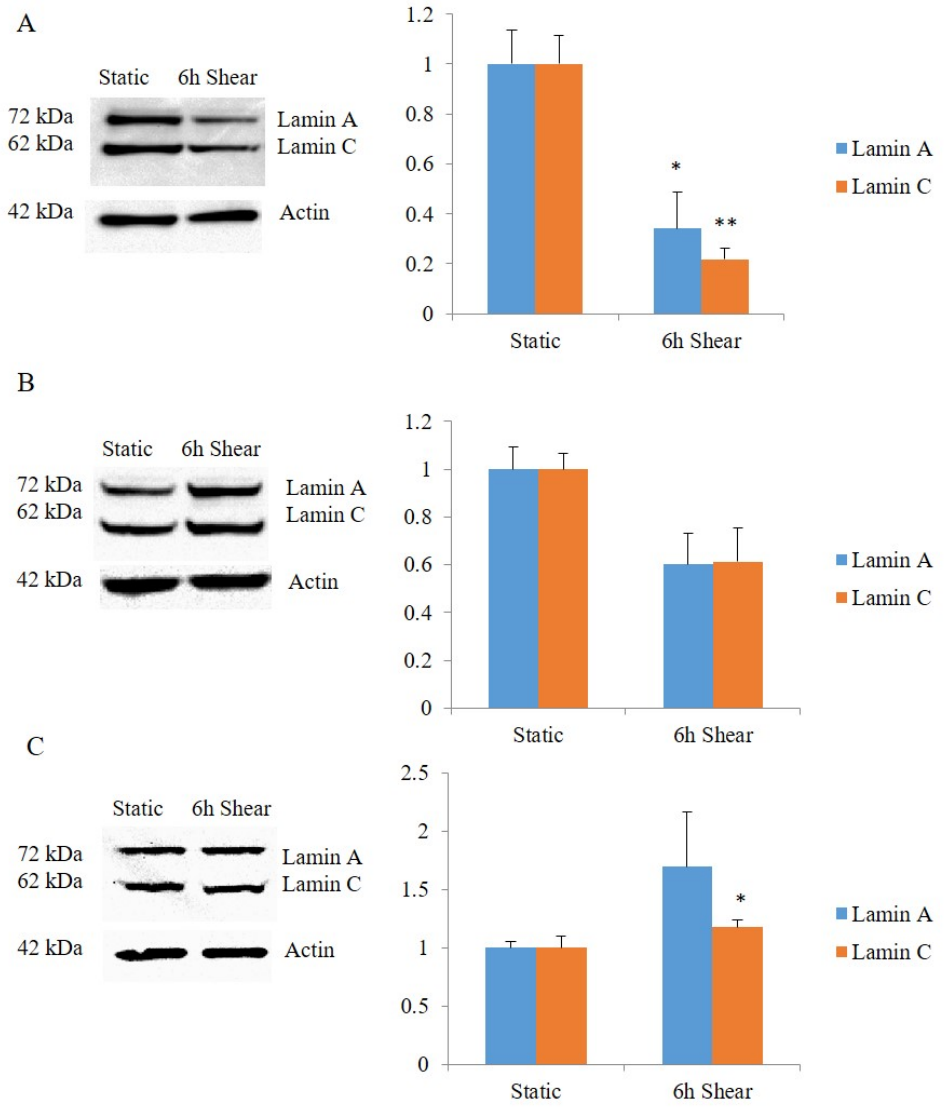

Fig. 3.4. Lamin A/C protein expression after 6-hour shear in cells in term of ages. **A.** Lamin A/C protein expression after 6-hour shear in young cells, which showed significant decreases compared to control sample (* $P < 0.05$ for lamin A and ** $P < 0.01$ for lamin C compared to control young cells). **B.** Lamin A/C protein expression after 6-hour shear in middle-age cells, and no significant value was observed. **C.** Lamin A/C protein expression after 6-hour shear in old cells, which showed significant increase for lamin C compared to control sample (*$P < 0.05$ compared to control old cells).

To verify western blot results, the mean intensity was quantified from immunostaining images, where lamin A/C antibody and its corresponding fluorophore conjugated secondary antibody were used to stain and visualize lamin A/C under fluorescent microscope. Results in Figure 3.5 shows consistent trends as in western blot. For young cells, the mean intensity was 15.92 ± 0.70, which significantly decreased to 13.53 ± 1.49 after shear (*** $P < 0.001$ compared to control young cells). For middle-age cells, the mean intensity was 12.37 ± 0.47 in static states, and after 6-hour shear it became 10.99 ± 0.72. For old cells, the mean intensities were 11.64 ± 0.46 and 16.37 ± 0.86 before and after shear, where it showed significantly increase (*** $P < 0.001$ compared to control old cells).

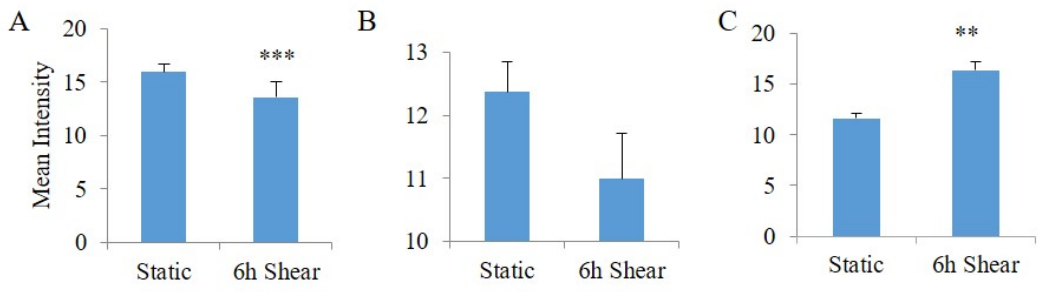

Fig. 3.5. Mean intensity of lamin A/C within the nucleus before and after shear for young **(A)**, middle **(B)** and old cells **(C)**. Cells were stained with lamin A/C antibody either in static condition or after 6-hour shear. 8 to 15 cells were picked for each analysis. Significant changes (*** $P < 0.001$ compared to control young cells) were observed for young cells, where it showed significant increase for old cells after shear. (** $P < 0.01$ compared with control old cells)

3.5 Nuclear Morphology Changes After 6-hour Shear in Young Cells

To further explore whether aging process influences nucleus shape, shear experiments were conducted on young, middle, old cells separately, and area, elongation and circularity were measured again, as Figure 3.6 shows. The area in static states was 2720.33 ± 92.70, 2939.17 ± 179.64, 3223.82 ± 180.56 for young, middle, old cells, respectively, while after shear the area became 2148.75 ± 91.32, 3334.30 ± 330.45, 3470.62 ± 151.61. For elongation, it was 1.02 ± 0.02, 0.91 ± 0.01 and 0.75 ± 0.01 in young, middle and old cells respectively under static states, and it became 1.11 ± 0.01, 0.89 ± 0.002, 0.74 ± 0.001 after shear experiments. For circularity, the value was 0.82 ± 0.01, 0.82 ± 0.02 and 0.81 ± 0.01 for young, middle and old control cells, and it became 0.84 ± 0.01, 0.80 ± 0.01 and 0.88 ± 0.01 after 6-hour shear.

So for young cells, shear stress decreased overall area significantly ($^{***}P < 0.001$ compared to control young cells). Nuclear area was not significantly changed for middle or old cells. Younger cell nuclei also had significantly increased elongation ($^{***}P < 0.001$ compared to control young cells). For middle aged cells, nuclear area, elongation, and circularity changed with shear stress, but the differences were not significant. Interestingly for old cells, shear stress did not change nuclear area or elongation. Only circularity increased significantly ($^{***}P < 0.001$ compared to control old cells).

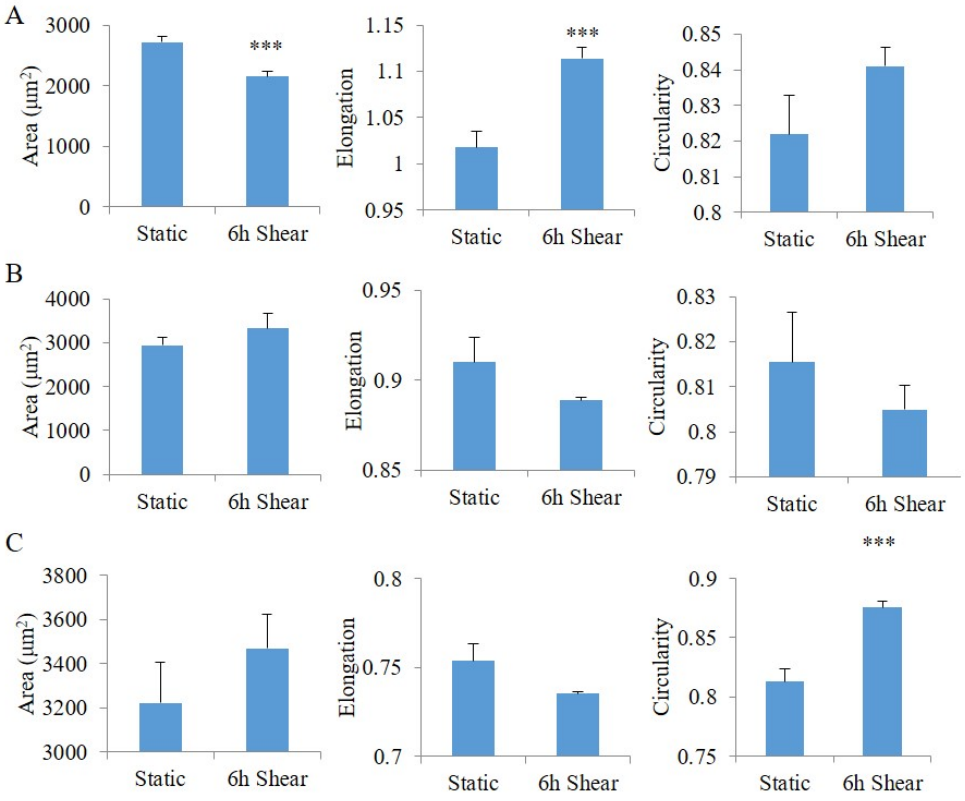

Fig. 3.6. Nuclear morphology analysis after shear for young **(A)**, middle **(B)** and old **(C)** cells. Cells were stained with lamin A/C antibody either in static condition or after 6-hour shear. 8 to 15 cells were picked for each analysis. The first, second and third columns represent area (μm^2), elongation and circularity, respectively. Significant changes (*** $P < 0.001$ compared to control young cells) were observed for young cells in area and elongation. The circularity was observed to increase significantly in old cells. (*** $P < 0.001$ compared to control old cells)

3.6 Old Cells Have Elevated mRNA Level of LMNA Gene After 6-hour Shear

To examine which expression level shear stress is acting on lamin A/C, Real time qPCR was utilized to investigate transcription level of lamin A/C after shear experiment. Figure 3.7 shows the RT-qPCR results. The threshold was detected for both LMNA primer and GAPDH primers in each sample, and Pfaffl method was utilized to calculate fold increases in sheared samples compared to samples in static state. After calculation, the fold increases of LMNA gene that encodes lamin A/C protein for young, middle, old cells after shear were 1.01 $\pm$ 0.02, 0.89 $\pm$ 0.02 and 1.43 $\pm$ 0.04, respectively, after normalized with GAPDH as control gene. Old cells show significant elevated transcription level of LMNA gene after 6-hour shear (* $P < 0.05$ compared to control old cells). For old cells this data is consistent with Western results.

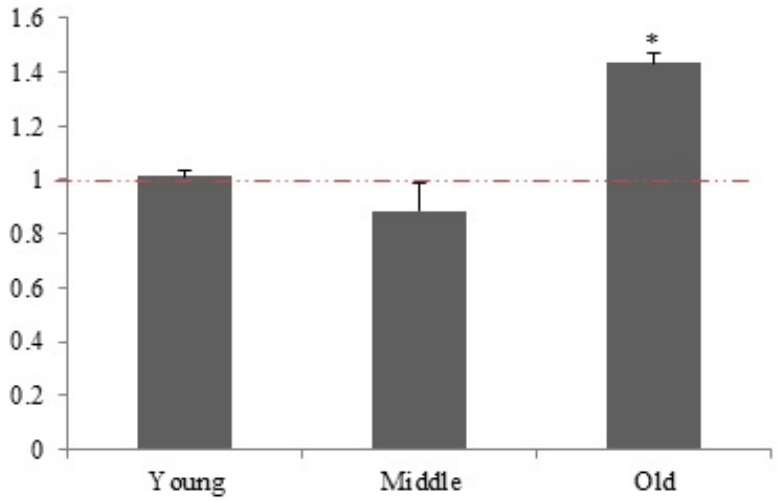

Fig. 3.7. Fold increase of LMNA (Lamin A/C) mRNA in BAEC after 6-hour shear through aging process. Old cells showed significantly higher transcription level of LMNA after shear stress (* $P < 0.05$ compared to control old cells).

3.7 Lamin A/C Accumulates at Nuclear Periphery After Shear, Especially in Young Cells

We also observed the distribution of the lamin proteins within the nucleus for static or sheared cells for young and older cells.

To quantify how lamin A/C locates within the nucleus and if shear stress regulates its distribution, analysis was performed to calculate the ratio of ratio of lamin A/C at periphery over the whole nucleus. Figure 3.8 shows representative images of stained young and old cells, in static or sheared condition, which show that lamin A/C is primarily localized at the nucleus, under static or shear condition. Based on these fluorescent images, quantitative analysis was carried out to measure nuclear periphery intensity over average nuclear intensity, and results are presented in Figure 3.9. The results show that the ratio increased after shear stress for all ages. We see a significant increase in lamin A/C at the nuclear peripheral for cells of all ages, significantly for young cells ($^{**}P < 0.01$ compared to young control cells, as in Figure 3.9A). The data for young, middle and old cells in static states were 0.85 ± 0.02, 0.88 ± 0.04 and 0.98 ± 0.02, respectively. After 6-hour shear, the ratios became 0.93 ± 0.02, 0.92 ± 0.02 and 1.03 ± 0.02 in young, middle and old cells, respectively.

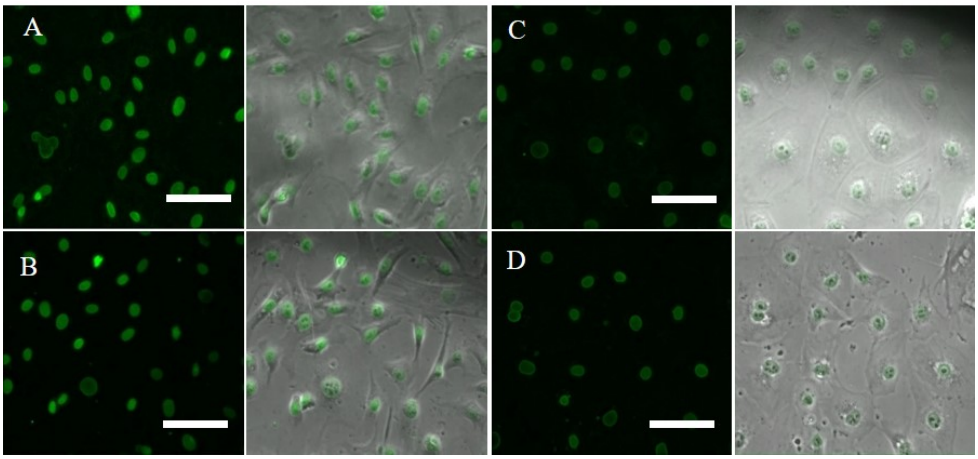

Fig. 3.8. Images of cells in static conditions (**A** and **C** represent young cells and old cells, respectively) or after 6-hour shear (**B** and **D** represent young cells and old cells, respectively). **A.** Young cells under static states. **B.** Young cells underwent 6-hour shear. **C.** Old cells under static states. **D.** Old cells underwent 6-hour shear. Each panel contains fluorescence (left) and merged images (right). Scale bar: 100 μm.

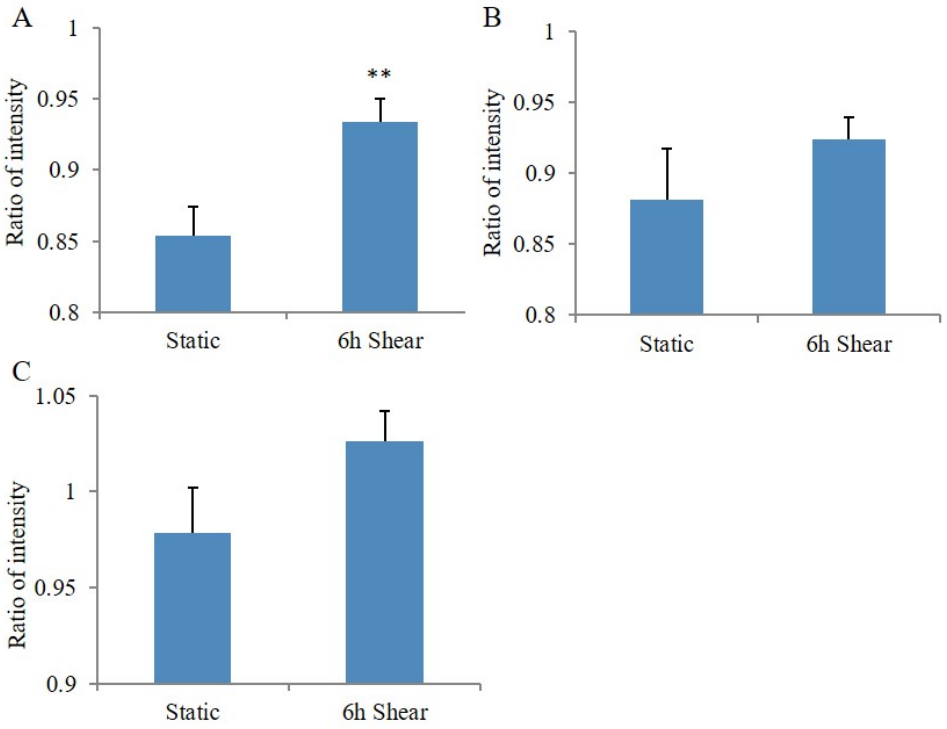

Fig. 3.9. Ratio of lamin A/C intensity at periphery over whole nucleus in static state or after 6-hour shear in young **(A)**, middle **(B)** and old **(C)** cells. Significant increase was observed in young cells after 6h shear ($^{**}P < 0.01$ compared to control young cells).

3.8 Lamin A/C Protein Expression Was Upregulated by Cyclic Stretch in Early Stages, but the Trend Dissipates in Old Cells

Endothelial cells not only sustain shear stress from blood flow, but also undergo a cyclic stretch produced by periodic distention and relaxing of arteries. Therefore, we investigated if lamin A/C would respond to a 10%, 1 Hz cyclic stretch and if aging process influences this potential regulation. Figure 3.10 shows that lamin A/C protein expression increased after 6-hour stretch in young cells (* $P < 0.05$ compared to control young cells), but it was not significant in middle cells. However, in old cells, the trend is opposite (** $P < 0.01$ compared to control old cells). After normalized to control, in young cells, the lamin A and lamin C expression levels were 1 ± 0.01 and 1 ± 0.04 respectively for control sample, and were 2.33 ± 0.29, 2.12 ± 0.23 for stretched samples. In middle cells, the expression levels in control samples were 1 ± 0.01 and 1 ± 0.06, in stretched samples the data were 1.57 ± 0.31 and 1.00 ± 0.30. In old cells, the protein expression levels for control samples were 1 ± 0.01 and 1 ± 0.18, whereas for stretched samples the data were 0.17 ± 0.05 and 0.16 ± 0.04. Our data suggests that cyclic stretch had very different, in fact opposite effects on lamin expression. Cells that were stretched were plated on stretchable silicone membrane, while for shear stress experiments, cells were plated on glass substrates. Glass is much stiffer than silicone, and silicone membranes had to be coated with fibronectin in order for cells to attach. Therefore, the differences in substrate stiffness as well as surface coating could be a contributing factor in the observed difference in lamin A/C expression.

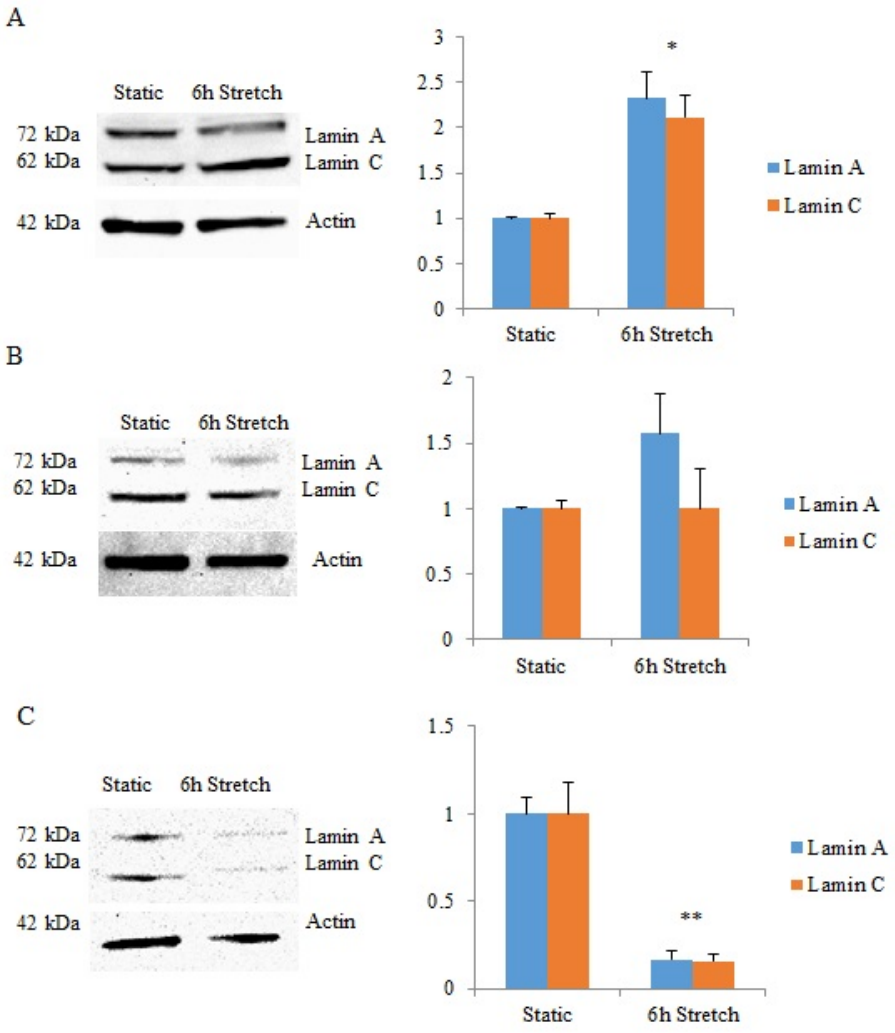

Fig. 3.10. Lamin A/C expression young **(A)**, middle **(B)** and old **(C)** cells under static condition or after 6-hour stretch. Younger cells had elevated lamin A/C expression levels after stretch (* $P < 0.05$ compared to control young cells), and lamin A/C failed to respond to stretch in middle cells, and were downregulated in old cells (** $P < 0.01$ compared to control old cells)

3.9 mRNA Level Was Upregulated in Cells of All Stages After 6-hour Stretch

RT-qPCR was performed to examine transcriptional changes in lamin A/C, as described previously. Figure 3.11 shows the fold changes of lamin A/C after 6-hour stretch at 10%, 1 Hz. The transcription levels for LMNA gene that encodes lamin A/C were upregulated in cells in young and old stages (* $P < 0.05$ compared to control young cells and control old cells, respectively). The fold increases of LMNA gene in young, middle and old cells were 1.94 ± 0.18, 1.29 ± 0.07 and 1.40 ± 0.09, respectively. Our data shows that the mRNA level for lamin A/C agrees with the protein expression levels. As the cells aged, both mRNA and protein expression levels decreased.

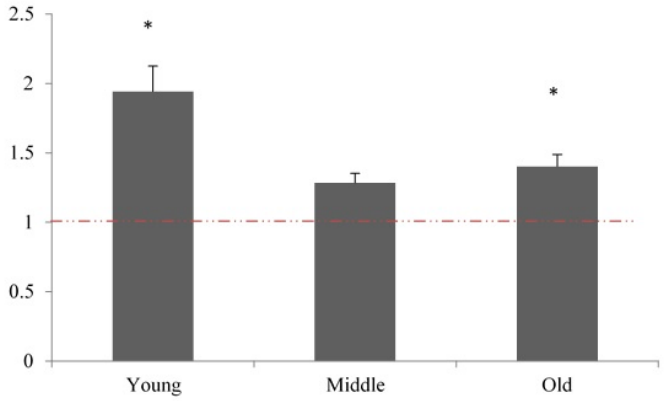

Fig. 3.11. Fold increases of LMNA (Lamin A/C) compared to GAPDH in BAEC after 6-hour stretch. In young and old cells, the transcription levels significantly increased. (* $P < 0.05$ compared to control young cells and control old cells, respectively).

3.10 Lamin A/C Distributed Differently with Age for Cells That Were Prepared for Cyclic Stretch

To visualize how lamin A/C locates in cells, immunostaining of lamin A/C antibody was used for young and old cells in either static state or after stretch, at 10%, 1 Hz cyclic stretch for 6 hour. Figure 3.12 shows cells in phase contrast or fluorescence images for static or stretched cells. Interestingly, results indicate that lamin A/C locates within the cytoplasm when cells are growing on silicone membrane coated with fibronectin, even before stretch, under static condition, especially in younger cells (Figure 3.12 A). This was unexpected since lamin A/C normally localize to the nucleus. Through the aging process, lamin A/C is shown to increasingly accumulate within the cytoplasm (Figure 3.12 C). After stretch, lamin A/C remained mostly cytoplasmic in younger cells while in older cells, lamin A/C has become mostly nuclear localized. Again, the differences in substrate stiffness as well as surface coating could have resulted the observed cytoplasmic lamin A/C. This is an unexpected and new finding, and more investigation is needed to better understand these results for cells prepared for stretch on silicone substrates.

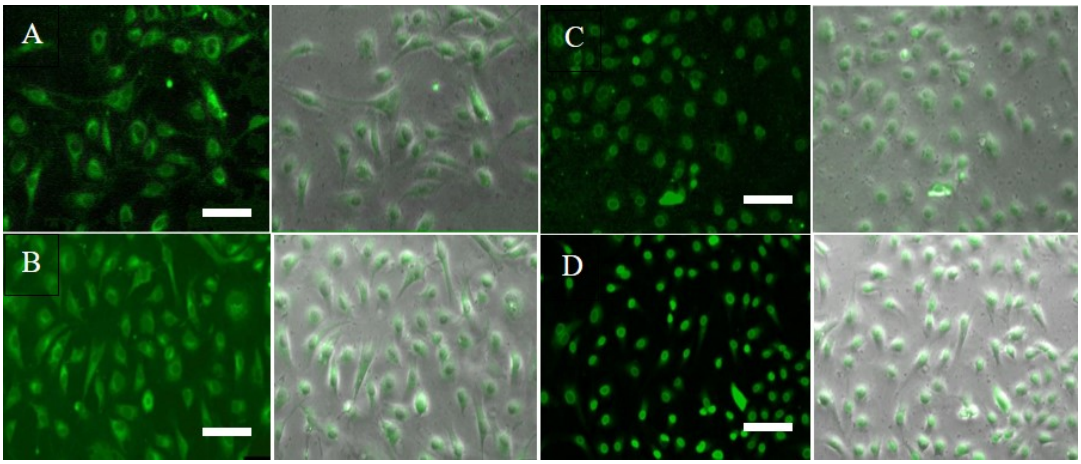

Fig. 3.12. Images of cells in static condition (**A** and **C**) or after 6-hour stretch (**B** and **D**). Each panel contains fluorescence and merged images. **A.** Young cells that were under static states. **B.** Young cells that underwent 6-hour stretch. **C.** Old cells that were under static states. **D.** Old cells that underwent 6-hour stretch. Scale bar: 75 μm.

4. DISCUSSION

4.1 The Expression of A-type Lamins Decreases as PDL Increases

Cell aging was indicated by population doubling level of PDL. As PDL increased, the lamin A/C expression decreased (see Figure 3.1). This is in good agreement with other researcher's observations [38]. Fluorescent images acquired by staining lamin A/C on glass slides indicated that, as cell grows older, A-type lamins become more localized to the nuclear lamina. Quantitative image analysis and statistical results showed that the ratio of lamin A/C at periphery and nucleoplasm is getting significantly higher in old cells than that of young cells (Figure 3.2). Therefore, the conclusion is that, through aging process, the overall expression of lamin A/C is suppressed, accompanying with its aggregation along the nuclear periphery.

4.2 The Response of Lamin A/C towards Shear Stress Varies in Young and Old Cells

The overall nuclear changes were first observed in endothelial cells after 6-hour shear, regardless PDL (see Figure 3.3). Overall, the nucleus was elongated along the orientation of laminar shear, and the nucleus area decreased after shear, which might come from the adjustment of nuclear lamina towards shear, as lamin A/C was downregulated after shear as well (data not shown here). However, when cells were divided into three groups as low PDL, middle PDL and high PDL to better evaluate cell age and its effect on lamin A/C, different regulation patterns of lamin A/C were observed (see Figure 3.4). Western blot showed that the lamin A/C were downregulated in young cells, however, the decreasing trend was not significant in cells with middle PDL, and was even reversed with high PDL. Further intensity results

from immunostaining (see Figure 3.5) verified Western blot results. At the same time, the morphological analysis indicates that the nuclear shape was not properly regulated in cells with higher DPL, as the area and elongation of nucleus did not change significantly in those cells after shear, which implicates the role of lamin A/C in modulating nuclear morphology (Figure 3.6). However, the circularity of cell nucleus was inconsistent with the previous overall circularity - the young and middle-age cells did not change much, while the old cells showed increased circularity. One explanation would be different immunostaining reagents used in separate experiments. In overall study, the nucleus was stained by Hoechst stain solution, which contains Hoechst dye that binds to DNA. But in later experiments with specific PDL, the nuclei were stained by lamin A/C antibody. Therefore, the latter one was more prone to delineating the nuclear periphery, which brought more details and variables into the circularity. Another concern is related to aging effect on endothelial cells, in which the old cells after shear gave smoother periphery of lamin A/C than static samples, whose lamin A/C network is irregular at some area, especially in old cells (See Figure 3.8 C and D). On another hand, the distribution of lamin A/C within nucleus also changed after 6-hour shear, especially in young cells, where the lamin A/C accumulated more at periphery after shear, which might contribute to the nucleus adjustment toward the mechanical force. However, this distribution was not significantly observed in middle and old cells (Figure 3.9), indicating an altered relocation of lamin A/C in aged cells during shear.

Moreover, the stable transcription level in cell with low DPL indicates that the transcription was not affected by shear stress, therefore, the downregulation effect in lamin A/C protein expression must happen after transcription, where either the mRNA or the protein was degraded by some regulators by the stimulation of laminar shear stress. Meanwhile, the transcription levels in aged cells after shear was actually increasing, indicating a potential regulation by transcription factors induced by shear stress (see Figure 3.7).

Overall, we investigated in details about how shear stress affects lamin A/C patterns, and demonstrate the hypothesis that aging process has an impact on the regulatory pathway for lamin A/C induced by laminar shear stress.

4.3 Lamin A/C Responds to Stretch Force in a Different Way Compared to Shear Stress

Endothelial cells seem to regulate lamin A/C differently when stretch force was applied. In young cells, the lamin A/C expression was promoted after 6-hour stretch (Figure 3.10). However, the upregulation dissipated again in middle-age cells, and was inversed in aged cells. As transcription levels were elevated in all stages, there seems to be some transcriptional regulation to promote the synthesis of lamin A/C mRNA in young cells when they experienced cyclic stretch, while post-transcriptional regulation is stimulated by the stretch to downregulate lamin A/C for aged cell(Figure 3.11).

Surprisingly, when visualization of lamin A/C was realized by staining cells with lamin A/C antibody, complete distinct distributions were observed in cells with varied DPL. In young cells, lamin A/C was shown to distribute more within cytoplasm instead of nucleus, but as PDL increases, lamin A/C is relocated back into nucleoplasm. In old cells, it was almost confined in nucleoplasm. Meanwhile, those distributions were intensified after 6-hour cyclic stretch. This rare phenomenon should not be an artifact, as cells at different ages were stained in the same way and at the same time. Therefore, the mechanism may come from the stiffness of the substrate, where silicone membrane coated with fibronectin was used instead of glass slide, or the coating fibronectin helps to form an unusual physical connection by lamin A/C during cell attachment. Further investigation is needed to further verify this observation.

5. CONCLUSIONS AND SUMMARY

5.1 Conclusions

Atherosclerosis is believed to be related to the mechanical forces exerted on vascular cells. Hemodynamic forces *in vivo*, including the shear stress generated by blood flow and the circumferential stretch force. These two forces are modulating vascular cells behaviors by regulating biological pathways. In this thesis, we mainly focused on how lamin A/C, one type of the structural and functional protein responds to hemodynamic forces for endothelial cells *in vitro*. Furthermore, aging process was taken into account to elaborate its role in regulating lamin A/C.

In this thesis, the possibility of lamin A/C regulation by mechanical forces was demonstrated, and aging process is found to be affecting how lamin A/C expression changes in response to applied forces. Although similar decreasing trend of lamin A/ expression was observed by aging and applying shear stress, their ultimate outcomes are different. While in aging process the nucleus shape is enlarged and cells are unable to adjust their morphology to adapt to external forces. Shearing on young cells promotes nuclear elongation as well as reduces nuclear area.

Furthermore, cyclic stretch may have completely different effects on lamin A/C expression in endothelial cells compared to shear stress. Distinct pathways may be involved under different mechanical stimulus, and under either shear or stretch, cell age is an important factor in lamin A/C expression and cellular localization. This project has shown that lamin A/C as a novel mechano-sensitive structural protein, whose expression and function is also affected by cell age. Exploring its upstream factors may shed a light in understanding how early atherosclerosis develops under hemodynamic forces and its relationship with aging process.

5.2 Future Work

As lamin A/C regulation levels have been confirmed, the next directions for shear stimulation would be to explore what regulators suppress lamin A/C protein expression after its transcription, if this regulation is disturbed in aged cells, as well as what transcription factors promotes lamin A/C mRNA synthesis after shear. Regarding stretch stimulation, future work will confirm lamin A/C localization in cells, on different substrate, as well as at different ages. Transcription factors involved in elevating lamin A/C mRNA expression are not yet identified. Further studies are needed to understand how lamin A/C is elevated in younger cells, but decreased in aged cells after stretch. This study will contribute to our understanding of nuclear defects in not only endothelial cells, but also in smooth muscle cells considering noticeable SMC loss in HGPS patients.

Moreover, this study will broaden to include detection of progerin, the mutated form of lamin A in HGPS cells, as it acts as a bridge between aging and lamin A/C mechanotransduction. As there is no cDNA sequence for progerin for bovine, a conversion to human endothelial cells is needed to further explore the function that progerin might have on normal lamin A/C expression pathways.

As for the unusual cytoplasmic distribution of lamin A/C in endothelial cells on silicone membranes coated with fibronectin, further experiments to explore its mechanism needs to be performed, and if lamin A/C is demonstrated to be able to function in cytoplasm, it may help to recognize novel functions of lamin A/C, which was thought to only exist in nucleus.

LIST OF REFERENCES

LIST OF REFERENCES

[1] T. Thom, N. Haase, W. Rosamond, V. J. Howard, J. Rumsfeld, T. Manolio, Z.-J. Zheng, K. Flegal, C. O'Donnell, S. Kittner, *et al.*, "Heart disease and stroke statistics–2006 update: a report from the american heart association statistics committee and stroke statistics subcommittee.," *Circulation*, vol. 113, no. 6, p. e85, 2006.

[2] M. J. Cipolla, "The cerebral circulation," *Integrated Systems Physiology: From Molecule to Function*, vol. 1, no. 1, pp. 1–59, 2009.

[3] M. W. Majesky, X. R. Dong, V. Hoglund, W. M. Mahoney, and G. Daum, "The adventitia a dynamic interface containing resident progenitor cells," *Arteriosclerosis, thrombosis, and vascular biology*, vol. 31, no. 7, pp. 1530–1539, 2011.

[4] J. F. Bentzon, F. Otsuka, R. Virmani, and E. Falk, "Mechanisms of plaque formation and rupture," *Circulation research*, vol. 114, no. 12, pp. 1852–1866, 2014.

[5] P. Libby, P. M. Ridker, and A. Maseri, "Inflammation and atherosclerosis," *Circulation*, vol. 105, no. 9, pp. 1135–1143, 2002.

[6] M. J. Thubrikar and F. Robicsek, "Pressure-induced arterial wall stress and atherosclerosis," *The Annals of thoracic surgery*, vol. 59, no. 6, pp. 1594–1603, 1995.

[7] G. D. Barish, A. R. Atkins, M. Downes, P. Olson, L.-W. Chong, M. Nelson, Y. Zou, H. Hwang, H. Kang, L. Curtiss, *et al.*, "Pparδ regulates multiple proinflammatory pathways to suppress atherosclerosis," *Proceedings of the National Academy of Sciences*, vol. 105, no. 11, pp. 4271–4276, 2008.

[8] A. J. Lusis, A. M. Fogelman, and G. C. Fonarow, "Genetic basis of atherosclerosis: part i new genes and pathways," *Circulation*, vol. 110, no. 13, pp. 1868–1873, 2004.

[9] K. J. Moore, V. V. Kunjathoor, S. L. Koehn, J. J. Manning, A. A. Tseng, J. M. Silver, M. McKee, and M. W. Freeman, "Loss of receptor-mediated lipid uptake via scavenger receptor a or cd36 pathways does not ameliorate atherosclerosis in hyperlipidemic mice," *The Journal of clinical investigation*, vol. 115, no. 8, pp. 2192–2201, 2005.

[10] A. I. Barakat and D. K. Lieu, "Differential responsiveness of vascular endothelial cells to different types of fluid mechanical shear stress," *Cell biochemistry and biophysics*, vol. 38, no. 3, pp. 323–343, 2003.

[11] J. Partridge, H. Carlsen, K. Enesa, H. Chaudhury, M. Zakkar, L. Luong, A. Kinderlerer, M. Johns, R. Blomhoff, J. C. Mason, *et al.*, "Laminar shear stress acts as a switch to regulate divergent functions of nf-κb in endothelial cells," *The FASEB Journal*, vol. 21, no. 13, pp. 3553–3561, 2007.

[12] Y.-X. Qi, J. Jiang, X.-H. Jiang, X.-D. Wang, S.-Y. Ji, Y. Han, D.-K. Long, B.-R. Shen, Z.-Q. Yan, S. Chien, *et al.*, "Pdgf-bb and tgf-β1 on cross-talk between endothelial and smooth muscle cells in vascular remodeling induced by low shear stress," *Proceedings of the National Academy of Sciences*, vol. 108, no. 5, pp. 1908–1913, 2011.

[13] N. Azuma, S. A. Duzgun, M. Ikeda, H. Kito, N. Akasaka, T. Sasajima, and B. E. Sumpio, "Endothelial cell response to different mechanical forces," *Journal of vascular surgery*, vol. 32, no. 4, pp. 789–794, 2000.

[14] H. Yoshisue, K. Suzuki, A. Kawabata, T. Ohya, H. Zhao, K. Sakurada, Y. Taba, T. Sasaguri, N. Sakai, S. Yamashita, *et al.*, "Large scale isolation of non-uniform shear stress-responsive genes from cultured human endothelial cells through the preparation of a subtracted cdna library," *Atherosclerosis*, vol. 162, no. 2, pp. 323–334, 2002.

[15] C. Ives, S. Eskin, and L. McIntire, "Mechanical effects on endothelial cell morphology: in vitro assessment," *In vitro cellular & developmental biology*, vol. 22, no. 9, pp. 500–507, 1986.

[16] J. B. Lansman, T. J. Hallam, and T. J. Rink, "Single stretch-activated ion channels in vascular endothelial cells as mechanotransducers?," 1987.

[17] M. A. Awolesi, W. C. Sessa, and B. E. Sumpio, "Cyclic strain upregulates nitric oxide synthase in cultured bovine aortic endothelial cells.," *Journal of Clinical Investigation*, vol. 96, no. 3, p. 1449, 1995.

[18] G. V. Letsou, O. Rosales, S. Maitz, A. Vogt, and B. E. Sumpio, "Stimulation of adenylate cyclase activity in cultured endothelial cells subjected to cyclic stretch.," *The Journal of cardiovascular surgery*, vol. 31, no. 5, pp. 634–639, 1989.

[19] P. F. Davies, "Flow-mediated endothelial mechanotransduction," *Physiological reviews*, vol. 75, no. 3, pp. 519–560, 1995.

[20] K. N. Dahl, A. J. Ribeiro, and J. Lammerding, "Nuclear shape, mechanics, and mechanotransduction," *Circulation research*, vol. 102, no. 11, pp. 1307–1318, 2008.

[21] R.-A. Rober, K. Weber, and M. Osborn, "Differential timing of nuclear lamin a/c expression in the various organs of the mouse embryo and the young animal: a developmental study," *Development*, vol. 105, no. 2, pp. 365–378, 1989.

[22] T. A. Dittmer and T. Misteli, "The lamin protein family," *Genome biology*, vol. 12, no. 5, p. 1, 2011.

[23] T. Shimi, K. Pfleghaar, S.-i. Kojima, C.-G. Pack, I. Solovei, A. E. Goldman, S. A. Adam, D. K. Shumaker, M. Kinjo, T. Cremer, *et al.*, "The a-and b-type nuclear lamin networks: microdomains involved in chromatin organization and transcription," *Genes & development*, vol. 22, no. 24, pp. 3409–3421, 2008.

[24] J. Lammerding, L. G. Fong, J. Y. Ji, K. Reue, C. L. Stewart, S. G. Young, and R. T. Lee, "Lamins a and c but not lamin b1 regulate nuclear mechanics," *Journal of Biological Chemistry*, vol. 281, no. 35, pp. 25768–25780, 2006.

[25] A. Muchir, J. Shan, G. Bonne, S. E. Lehnart, and H. J. Worman, "Inhibition of extracellular signal-regulated kinase signaling to prevent cardiomyopathy caused by mutation in the gene encoding a-type lamins," *Human molecular genetics*, vol. 18, no. 2, pp. 241–247, 2009.

[26] L. J. Emerson, M. R. Holt, M. A. Wheeler, M. Wehnert, M. Parsons, and J. A. Ellis, "Defects in cell spreading and erk1/2 activation in fibroblasts with lamin a/c mutations," *Biochimica et Biophysica Acta (BBA)-Molecular Basis of Disease*, vol. 1792, no. 8, pp. 810–821, 2009.

[27] K. Tilgner, K. Wojciechowicz, C. Jahoda, C. Hutchison, and E. Markiewicz, "Dynamic complexes of a-type lamins and emerin influence adipogenic capacity of the cell via nucleocytoplasmic distribution of β-catenin," *Journal of cell science*, vol. 122, no. 3, pp. 401–413, 2009.

[28] S. Vlcek and R. Foisner, "A-type lamin networks in light of laminopathic diseases," *Biochimica et Biophysica Acta (BBA)-Molecular Cell Research*, vol. 1773, no. 5, pp. 661–674, 2007.

[29] R. Pollex and R. Hegele, "Hutchinson–gilford progeria syndrome," *Clinical genetics*, vol. 66, no. 5, pp. 375–381, 2004.

[30] C. L. Stewart, S. Kozlov, L. G. Fong, and S. G. Young, "Mouse models of the laminopathies," *Experimental cell research*, vol. 313, no. 10, pp. 2144–2156, 2007.

[31] D. McClintock, D. Ratner, M. Lokuge, D. M. Owens, L. B. Gordon, F. S. Collins, and K. Djabali, "The mutant form of lamin a that causes hutchinson-gilford progeria is a biomarker of cellular aging in human skin," *PloS one*, vol. 2, no. 12, p. e1269, 2007.

[32] C. D. Ragnauth, D. T. Warren, Y. Liu, R. McNair, T. Tajsic, N. Figg, R. Shroff, J. Skepper, and C. M. Shanahan, "Prelamin a acts to accelerate smooth muscle cell senescence and is a novel biomarker of human vascular aging," *Circulation*, vol. 121, no. 20, pp. 2200–2210, 2010.

[33] P. Scaffidi and T. Misteli, "Lamin a-dependent nuclear defects in human aging," *Science*, vol. 312, no. 5776, pp. 1059–1063, 2006.

[34] J. Afilalo, I. A. Sebag, L. E. Chalifour, D. Rivas, R. Akter, K. Sharma, and G. Duque, "Age-related changes in lamin a/c expression in cardiomyocytes," *American Journal of Physiology-Heart and Circulatory Physiology*, vol. 293, no. 3, pp. H1451–H1456, 2007.

[35] G. Duque and D. Rivas, "Age-related changes in lamin a/c expression in the osteoarticular system: laminopathies as a potential new aging mechanism," *Mechanisms of ageing and development*, vol. 127, no. 4, pp. 378–383, 2006.

[36] J. Lammerding, P. C. Schulze, T. Takahashi, S. Kozlov, T. Sullivan, R. D. Kamm, C. L. Stewart, and R. T. Lee, "Lamin a/c deficiency causes defective nuclear mechanics and mechanotransduction," *The Journal of clinical investigation*, vol. 113, no. 3, pp. 370–378, 2004.

[37] C. Guilluy, L. D. Osborne, L. Van Landeghem, L. Sharek, R. Superfine, R. Garcia-Mata, and K. Burridge, "Isolated nuclei adapt to force and reveal a mechanotransduction pathway within the nucleus," *Nature cell biology*, vol. 16, no. 4, p. 376, 2014.

[38] Y. Han, L. Wang, Q.-P. Yao, P. Zhang, B. Liu, G.-L. Wang, B.-R. Shen, B. Cheng, Y. Wang, Z.-L. Jiang, *et al.*, "Nuclear envelope proteins nesprin2 and lamina regulate proliferation and apoptosis of vascular endothelial cells in response to shear stress," *Biochimica et Biophysica Acta (BBA)-Molecular Cell Research*, vol. 1853, no. 5, pp. 1165–1173, 2015.

[39] J. Swift, I. L. Ivanovska, A. Buxboim, T. Harada, P. D. P. Dingal, J. Pinter, J. D. Pajerowski, K. R. Spinler, J.-W. Shin, M. Tewari, *et al.*, "Nuclear lamin-a scales with tissue stiffness and enhances matrix-directed differentiation," *Science*, vol. 341, no. 6149, p. 1240104, 2013.

[40] K. Rennier, *The role of DAP-kinase in modulating vascular endothelial cell function under fluid shear stress*. PhD thesis, 2015.

[41] F. Paul Jr *et al.*, *Tissue Culture: Methods and Applications*. Elsevier, 2012.

[42] Wikipedia, "Dna separation by silica adsorption — wikipedia, the free encyclopedia." `https://en.wikipedia.org/w/index.php?title=DNA_separation_by_silica_adsorption&oldid=633325966`, 2014. [Online; accessed 22-July-2016].

[43] M. Hunt, "Real Time PCR." `http://www.microbiologybook.org/pcr/realtime-home.htm`, 2010. [Online; accessed 1-Feb-2016].

[44] M. W. Pfaffl, "A new mathematical model for relative quantification in real-time rt–pcr," *Nucleic acids research*, vol. 29, no. 9, pp. e45–e45, 2001.

[45] A. Biosystems, *Guide to Performing Relative Quantitation of Gene Expression Using Real-Time Quantitative PCR*.

[46] R. Thavarajah, V. K. Mudimbaimannar, J. Elizabeth, U. K. Rao, K. Ranganathan, *et al.*, "Chemical and physical basics of routine formaldehyde fixation," *Journal of Oral and Maxillofacial Pathology*, vol. 16, no. 3, p. 400, 2012.

[47] J. T. Philip and K. N. Dahl, "Nuclear mechanotransduction: response of the lamina to extracellular stress with implications in aging," *Journal of biomechanics*, vol. 41, no. 15, pp. 3164–3170, 2008.